



**Aalto University
School of Chemical
Engineering**

Noora Raipale

IMPROVING STRENGTH AND RESILIENCE OF FOAM-FORMED FIBRE CUSHIONING

Master's Programme in Chemical, Biochemical and Materials Engineering
Major in Fibre and Polymer Engineering

Master's thesis submitted for examination for the degree of
Master of Science in Technology
Espoo, 11th July 2022

Supervisor	Prof. Jouni Paltakari
Advisors	M.Sc. (Tech) Elina Pääkkönen, M.Sc. Tiinamari Seppänen

Copyright ©2022 Noora Raipale

Author Noora Raipale

Title of thesis Improving strength and resilience of foam-formed fibre cushioning

Programme Chemical, Biochemical and Materials Engineering

Major Fibre and Polymer Engineering

Thesis supervisor Prof. Jouni Paltakari

Thesis advisor(s) M.Sc. (Tech) Elina Pääkkönen, M.Sc. Tiinamari Seppänen

Collaborative partner VTT

Date 11.07.2022 **Number of pages** 72 + 14 **Language** English

Abstract

Sustainability has become one of the key factors driving in the decision of materials for different applications. In package cushioning, new environmentally friendly alternatives are needed to reduce the use of non-renewable polymeric foams. Fibre-based foam-formed cushioning materials are promising alternatives to replace some of the petroleum-based materials.

In this work, the aim was to improve strength and resilience of foam-formed structures with various chemicals. Bleached chemi-thermomechanical pulp (BCTMP) fibres were used together with non-ionic foaming agent (AG6210) as a base structure for foam-formed materials with a target density of 60 kg/m³. The dynamic shock cushioning results from mechanical testing, Platen drop test, showed that the samples including chitosan and synthetic latex resulted in the highest maximum G values together with the highest resilience. Micro-computed X-ray tomography and Scanning Electron Microscopy (SEM) images showed variation in the internal structures of different samples; more homogeneous structures with smaller and more even pore size distribution performed better in general. However, more research is needed to understand the causality better.

Keywords foam forming, foam technology, cellulose, cushioning, packaging, strength, resilience



Tekijä Noora Raipale

Työn nimi Vaahtorainattujen kuiturakenteiden lujuuden ja palautuvuuden parantaminen

Koulutusohjelma Chemical, Biochemical and Materials Engineering

Pääaine Fibre and Polymer Engineering

Vastuopettaja/valvoja Professori Jouni Paltakari

Työn ohjaaja(t) DI Elina Pääkkönen, FM Tiinamari Seppänen

Yhteistyötaho VTT

Päivämäärä 11.07.2022 **Sivumäärä** 72 + 14 **Kieli** englanti

Tiivistelmä

Kestävästä kehityksestä on tullut yksi avaintekijöistä valittaessa materiaaleja eri sovelluksiin. Pakkauspehmusteiksi tarvitaan uusia ympäristöystävällisiä vaihtoehtoja uusiutumattomien polymeerivaahtojen käytön vähentämiseksi. Vaahtorainatut kuitumateriaalit ovat yksi lupaava vaihtoehto korvaamaan osan fossiilipohjaisista materiaaleista.

Tässä työssä tarkoituksena oli parantaa vaahtorainattujen kuiturakenteiden lujuutta ja palautuvuutta eri kemikaalien lisäyksellä. Pohjamateriaalina käytettiin valkaistua kemitermomekaanista massaa (BCTMP) yhdessä nonionisen vaahdotusaineen (AG6210) kanssa, ja lopputuotteiden tavoitetiheys oli 60 kg/m^3 . Dynaamiset iskunvaimennustulokset mekaanisesta testistä, ”Platen drop test”, osoittivat, että kitosaania ja synteettistä lateksia sisältävät näytteet johtivat korkeimpiin maksimi G-arvoihin yhdessä parhaimman palautuvuuden kanssa. Mikrotietokoneröntgentomografia- ja pyyhkäisyelektronimikroskoopi (SEM) -kuvat osoittivat vaihtelua eri näytteiden sisärakenteissa; homogeenisimmät rakenteet, joissa oli pienempi ja tasaisempi huokoskokojakauma, johtivat yleisesti parempaan lujuuteen ja palautuvuuteen. Lisätutkimusta kuitenkin vielä tarvitaan, jotta vaikutuksia ymmärretään paremmin.

Avainsanat vaahtorainaus, vaahtoteknologia, selluloosa, pehmustemateriaali, pakkaus, lujuus, palautuvuus

PREFACE

This master's thesis was carried out at VTT Technical Research Centre of Finland Ltd, as a part of the Piloting Alternatives for Plastics (PAfP) project. The research aims to develop new value-added fibre-based materials to replace plastics. This master's thesis was done between January 2022 and July 2022, and the experimental work was performed at VTT Jyväskylä during spring 2022.

I want to express my appreciation to my supervisor, Prof. Jouni Paltakari and advisors, Elina Pääkkönen and Tiinamari Seppänen, for guidance, support, and trust together with highly insightful feedback throughout the whole project, I could not have asked more.

Additionally, I want to thank the technical research team of VTT Jyväskylä and VTT Espoo, and all the people that introduced me to laboratory work together with other guidance. I appreciate all of your help, expert knowledge and discussions that guided me to finish the experiments together with analyzing the results.

From the bottom of my heart, I want to thank my family and friends for your support and encouraging words throughout my studies at Aalto University and especially during this thesis project. Thank you for being there when needed.

Vantaa, 11.07.2022

Noora Raipale

TABLE OF CONTENTS

PREFACE	
SYMBOLS AND ABBREVIATIONS	
1 INTRODUCTION.....	2
LITERATURE REVIEW	4
2 FOAM FORMING	4
2.1 Foams.....	4
2.2 Foam forming process.....	7
2.3 Foam-formed structures	10
3 CUSHIONING PROPERTIES	11
3.1 Traditional cushioning materials	12
3.2 Fragility of packed items.....	13
3.3 Mechanical testing of low-density materials.....	13
3.3.1 Platen drop test.....	14
3.3.2 Cushion curve	15
4 STRENGTH PROPERTIES.....	17
4.1 Factors affecting the strength of foam-formed structures.....	18
4.2 Factors affecting compression recovery	19
5 ADDITIVES TO IMPROVE STRENGTH PROPERTIES.....	20
5.1 Cellulose nanofibrils (CNF)	21
5.2 Polyvinyl alcohol (PVA)	22
5.3 Guar gum.....	23
5.4 Carrageenan	24
5.5 Agar	25
5.6 Cationic starch	26
5.7 Chitosan.....	27
5.8 Natural rubber	28
5.9 Crosslinkers	28
5.10 Retention aids	29
6 CHARACTERIZATION METHODS	29
6.1 Micro-computed X-ray tomography (μ XRT).....	30
6.2 SEM Imaging	30

7	ENVIRONMENTAL ASPECTS	31
	EXPERIMENTAL PART	32
8	MATERIALS.....	32
9	METHODS	35
9.1	Sample preparation.....	35
9.2	Sample testing	38
9.3	Sample characterization.....	38
10	RESULTS.....	39
10.1	Foaming and sample structure.....	39
10.2	Drop test results – Strength and resilience	40
10.3	Drop test results – failure modes.....	48
10.4	Results of micro-computed X-ray tomography.....	49
10.4	Results of porosity profile and pore size distribution	54
10.5	Results of SEM imaging.....	56
11	DISCUSSION	58
11.1	Effect of homogeneity and even distribution of fibres on the results	58
11.2	Results of strength and resilience compared to EPS and PU	59
11.3	The effect of different additives on strength and resilience	60
11.4	Potential replacement of cushioning materials	64
11.5	Challenges and uncertainties	65
12	CONCLUSION.....	66
	REFERENCES.....	68
	APPENDICES	74

SYMBOLS AND ABBREVIATIONS

Symbols

A	surface area
a_m	maximum acceleration
g	acceleration of gravity
G_c	fragility
m	mass
rpm	rounds per minute
W	plate weight
wt. %	weight percentage
Φ	liquid fraction
σ_s	static stress

Abbreviations

aPAM	anionic acrylamide copolymer
(B)CTMP	(bleached) chemithermomechanical pulp
CH ₃ OH	methanol
CNF	cellulose nanofibrils
cPAM	cationic acrylamide copolymer
DP	degree of polymerization
EPS	expanded polystyrene
FE-SEM	field-emission scanning electron microscope
HefCel	high-consistency enzymatically fibrillated cellulose

NaOH	sodium hydroxide
NFC	nanofibrillated cellulose
PAE	polyamine epichlorohydrin
PEO	polyethylene oxide
PP	polypropylene
PS	polystyrene
PU	polyurethane
PVA	polyvinyl alcohol
PVC	polyvinyl chloride
RH	relative humidity
SEM	scanning electron microscope
μXRT	micro-computed X-ray tomography

1 INTRODUCTION

Global packaging market has increased enormously during the last years and is expected to grow over the next decade. At the same time, concern over the environmental impact of packaging materials has risen. Sustainability has become one of the key factors that drive both, brands and customers, to choose packaging materials more ecologically, showing the commitment to the environment. Due to the growing demand for packaging solutions, it is crucial to replace materials from petrochemicals with new and sustainable sources.

In the transportation of a product, the packaged products face a variety of mechanical stress, such as compression, vibration, and sudden shocks, such as an accidental drop of the product, thus the product must be protected well from damages. Lightweight materials are used especially in cushioning of the packaging to protect products from damages in the transporting process from manufacturing to a final destination. Traditional lightweight materials that are used in cushioning are e.g., expanded polystyrene (EPS), polyurethane (PU) and phenolic foams (Landrock, 1995). The foam forming technique of low-density materials that are made from natural fibres is one solution to replace some of these fossil fuel -based packaging or cushioning materials (Burke et al., 2021; Hjelt et al., 2021; Poranen et al., 2013).

In the traditional papermaking process, foam and excess air have been seen more as a problem and more foam controlling agents have been investigated than foaming agents (Kidner, 1974). In the 1970s, The Radfoam process was developed, and it was used in non-woven industry, to produce specialized bulky papers (Kidner, 1974; Punton, 1975). This process resulted in high sheet uniformity and made it possible to handle longer, fibrillated fibres that were not shortened in the refining process (Kidner, 1974; Punton, 1975). The Radfoam process is better known as a foam forming process nowadays, so foam forming is not a totally new technique, but it was forgotten for some time until value-added fibre products started to be under interest (Kinnunen et al., 2013).

In this thesis, the focus is on the improvement of the strength and resilience of foam-formed structures. This thesis aims at answering the following research questions:

How can strength and resilience be maximized in foam-formed structures?

What are the main factors that affect strength and resilience of low-density fibrous structures?

How different additives affect strength and resilience of foam-formed fibre cushioning?

In the second chapter, the basics of foams and foam forming technique are explained. Then, in the third chapter, the discussion continues by explaining traditionally used cushioning materials, cushioning properties, and testing of cushioning properties. In the fourth chapter, several factors affecting the strength properties and resilience of foam-formed structures are explained. In the fifth chapter are listed and explained different additives that could potentially improve the strength properties of foam-formed structures. In the sixth chapter the characterization methods that were used in the further analysis of the mechanical testing results, X-ray micro-computed tomography, and SEM imaging, are briefly explained. Finally, in the seventh chapter, environmental aspects regarding cushioning materials are shortly explained.

The meaning of the research was to study, whether the addition of different additives increases the strength and resilience of foam-formed fibrous structures, and what is the optimal amount to maximize strength and resilience. The additives were chosen according to possible strengthening mechanisms that can occur when added to the foam-formed structure. The hypothesis is that for most additives, the reinforcement mechanism is based on the formation of hydrogen or other bonds between groups in additives and hydroxyl groups of cellulose fibres, or gathering of polymers into the fibre joints, which eventually strengthens the fibrous network. In some trial points, a crosslinker or retention aid was used to see if it aids the additives to improve the strengthening mechanism more or increase the retention rate of additives in the final structure. The strength and resilience of samples were tested with Platen drop test, and the obtained results were interpreted

together with characterization results from X-ray micro-computed tomography, and SEM imaging.

LITERATURE REVIEW

2 FOAM FORMING

2.1 Foams

Foam is commonly described as a dispersed system of gas bubbles in a continuous phase, in which the volume fraction of gas is higher than the volume fraction of a continuous phase (Atri & Ashrafizadeh, 2010). Foams are used in many applications, such as in construction, packaging, cushioning, insulation, foods, and biomedical fields (di Maio et al., 2021). Foams can be separated into liquid and solid foams. The liquid content determines the type of foam. In liquid foam, the liquid is a continuous phase in which gas is dispersed in, and in solid foams, gas is dispersed in a gel or a solid phase (di Maio et al., 2021; Langevin, 2017). Solid foams can be further classified into two different structures, open and closed cell foams. In open-cell structures, the gas pockets inside the foam are connected and form an interconnected network (Exerowa & Kruglyakov, 1998). In closed-cell foams, the gas pockets are not connected and have borders in between (Exerowa & Kruglyakov, 1998).

The liquid foams can be further classified into wet foams, dry foams, and bubbly liquids depending on the liquid fraction Φ , that is the ratio of the total volume of the gas bubbles, foam, and total volume of the continuous phase, liquid (Weaire & Hutzler, 1999). The shape of the bubbles differs between the wet and dry foams, depending on the liquid fraction of the foam system (Figure 1). In dry foams, the liquid fraction is lower resulting in the polyhedral shape of the bubbles, whereas when the liquid content is increased, the bubbles are shaped more into spherical structures, and this is common for wet foams (Weaire & Hutzler, 1999). When the liquid content still increases, the liquid fraction of the foam is increased above the critical liquid fraction, Φ_c , which is around 36%, and the foam system is classified as a bubbly liquid (Weaire & Hutzler, 1999). In this state, the bubbles are shaped almost completely spherical, and the gas bubbles are more separated and

flow easier in the liquid phase. The state in which the shape of the bubbles changes from polyhedral to spherical and bubbles are more free to move is described as a jamming transition (Weaire & Hutzler, 1999).

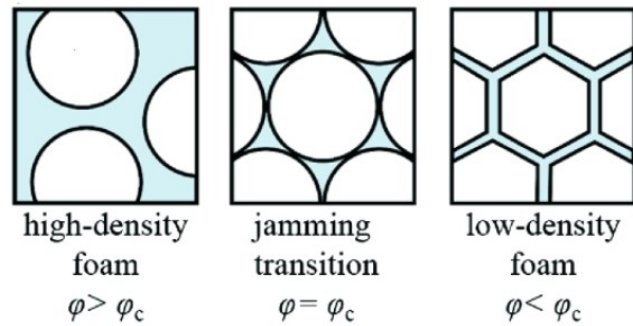


Figure 1. The shape of the bubbles depends on the liquid content of foam structure: (a) bubbly liquid ($\Phi > 36\%$), (b) transition from bubbly liquid to wet foam ($\Phi = 36\%$), (c) wet foam ($\Phi < 36\%$). (Andrieux, 2019)

Liquid foams are naturally not stable, so foaming agents, or surfactants, are needed to stabilize the foams. Surfactants are amphiphilic molecules meaning that they are partly hydrophilic (water-soluble) and partly hydrophobic (soluble in lipids). Surfactants consist of a hydrophilic group that is attached to a hydrophobic tail. In foams, surfactants adsorb at the gas-liquid interface creating elastic films that stabilize the air bubbles and prevent bubbles from collapsing (Figure 2). (Schramm & Wassmuth, 1994)

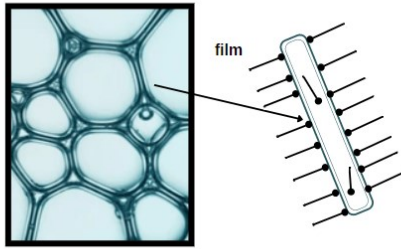


Figure 2. Aqueous foam is stabilized by surfactants. Surfactants adsorb on the liquid-bubble interface, polar heads are in contact with water, and hydrophobic tails are in contact with air bubbles. Adapted illustration from Bureiko et al., 2015.

Foam stability and foamability depend highly on the type and concentration of the used surfactant. When generating the foam, the surface area of liquid increases and surface energy also increases (Schramm & Wassmuth, 1994). According to Gibbs' minimum free energy principle, the system tends to go to a lower surface energy state, so naturally the bubbles would collapse (Callen, 1991). The addition of foaming agents reduces the interfacial tension between gas and liquid phases, i.e., decreasing the collapse of the bubbles (Schramm & Wassmuth, 1994). Surfactants also increase the surface viscosity of the foams forming more stable foams. (Schramm & Wassmuth, 1994)

Other factors that affect the foam stability are e.g., temperature, solution viscosity, bubble size distribution, and half-life time of the foam. An increase in temperature usually reduces the stability of foams by decreasing the viscosity of the solution. Higher solution viscosity can be obtained with the addition of some additives, for example, water-soluble polymers or gelling agents, that will reduce the drainage of the foam. The half-life time of foam is defined as the time required for 50% of the volume of the aqueous medium used in the foam to drain and revert to the liquid phase. The longer the half-time, the higher the stability of the foam. (Roy Choudhury, 2013)

A structure of a dry foam's interface in two dimensions (2D) is presented in Figure 3. The gas bubbles are separated by thin-film regions, that are formed from the liquid phase, and the faces of the thin film regions are called lamellae. The corners in which three lamellae meet are called Plateau borders, which are the points in which the liquid flow is the highest. In dry foams, Plateau borders are at angles of 120° resulting in a polyhedral

shape of the bubbles. In three dimensions, the angle at which four Plateau borders meet is approximately 109° . Without the use of surfactants, the structure of the foam continually changes, since the flow of the liquid is higher through the continuous network of Plateau borders, and the coalescence occurs fast between the gas bubbles. When using a surfactant, the surfactant adsorbs at the gas-liquid interface stabilizing the thin-film between the two interfaces resulting in a stable foam and decreasing the coalescence of the bubbles. (Schramm & Wassmuth, 1994)

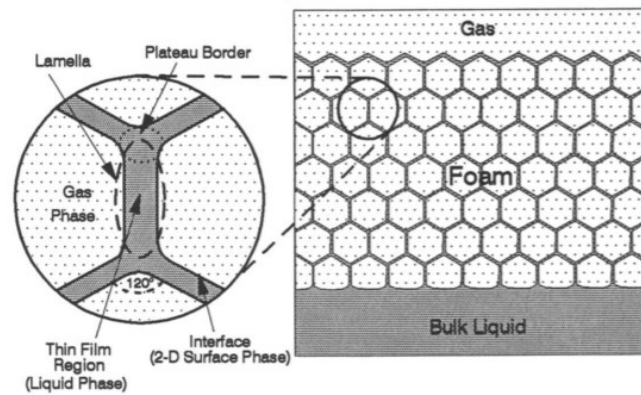


Figure 3. An illustration of dry foam's structure. (Schramm & Wassmuth, 1994)

2.2 Foam forming process

In the traditional papermaking process, fibrous material is dispersed in water to form an oriented two-dimensional network, and efficient air removal is needed in different unit operations. In this process, water acts as a transfer medium, but also as a glue to bind cellulose fibres together, and this results in strong and light material that has many applications. One problem with water's ability to bind hygroscopic cellulose fibres together is the flocculation of the fibres. Flocculation occurs when the fibres encounter high shear forces, and the fibres start to bend and rotate and get attached forming flocs. Flocculation of fibres affects the fibre distribution, which becomes uneven because of bundled fibres. To create materials with high strength properties, uniform fibre distribution and structure are important, since bundled fibres reduce the contact area and bonds

between the fibres and the surrounding medium that decreases the total strength of the material. (Hjelt et al., 2021; Punton, 1975)

Flocculation can be prevented in a few ways. One solution is to reduce the fibre concentration below the critical concentration, that is the concentration above which the fibres start to collide and flocculate. The other solution is to increase the viscosity of the suspending medium. Increased viscosity decreases the flow of the fibres reducing the likelihood of fibres colliding and forming bundles. (Hjelt et al., 2021; Punton, 1975)

In the 1970s, when foam forming technology, or the Radfoam process, was first developed, the process was originally a by-product of a papermaking research. However, it was soon realized, that even long fibres can be used to produce structures with uniform fibre distribution (Punton, 1975). Since most of the suspending medium was air, the drainage of water was faster, and this new technique offered a solution to some problems, e.g., flocculation when using long fibres, and air became an advantage in papermaking to create new functionalities and possibilities for fibrous structures (Punton, 1975).

The foam produced by foam forming technology is characterized as a wet foam, and it contains small spherical air bubbles with about 20-200 μm in diameter (Kinnunen et al., 2013, Punton, 1975). When the goal is to produce porous and lightweight structures, air content must be high. The air content in foam forming is usually 60-70 %, but some studies have revealed that foam forming works also with lower, 30-40%, air content (Lehmonen et al., 2020). Foams that are classified as liquid foams have pseudoplastic characteristic that is advantageous in the foam forming process - the foams have high viscosity at low shear rates and low viscosity at high shear rates (Kinnunen et al., 2013). Liquid foams allow the use of long fibres which is not convenient in the traditional papermaking process, since higher viscosity is needed when using long fibres to prevent flocculation of the fibres, and increased viscosity slows down the drainage, which also affects the speed of production (Punton, 1975).

In the foam forming process, water is still used as a transfer medium and as a glue to bind cellulose fibres to form a uniform network, but the flocculation is prevented by air bubbles that decrease the mobility of the fibres leading to a more homogeneous structure (Figure 4) (Kidner, 1974; Lehmonen et al., 2020; Punton, 1975). Air bubbles also prevent the possibility of fibres attaching to surrounding fibre walls, since fibres are surrounded

by foam, which decreases the entanglement or flocculation of the fibres (Kidner, 1974; Lehmonen et al., 2020; Punton, 1975). Because of these characteristics, long fibres can be used to produce fibrous structures with excellent formation. In the traditional papermaking process, it is more common to use short and stiff wood fibres, since using long fibres increases the risk of collision and flocculation of the fibres in wet web forming (Kidner, 1974; Lehmonen et al., 2020; Punton, 1975).

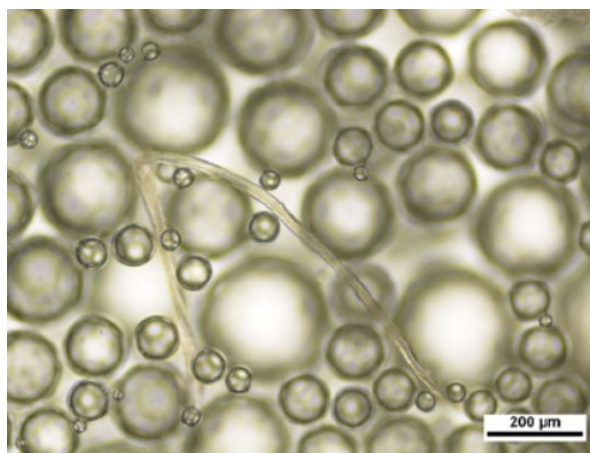


Figure 4. A wood fibre surrounded by bubbles in the foam. Bubbles attach to the fibre walls preventing flocculation. (Lehmonen et al., 2020)

In the Radfoam process, the air content varied between 55 and 75%, and fibres were used together with aqueous foam (Smith et al., 1974). The idea of the foam was to bind fibres to air bubbles to decrease the mobility of the fibres (Smith et al., 1974). This resulted in a more uniform and stable structure that could be confirmed with characterization methods that revealed more uniform mass density distribution, smoother surface, and increased bulk and porosity compared with comparable water-laid structures (Punton, 1975; Smith & Punton, 1975). One downside of the process was the lower strength of foam-laid structures compared with the strength of water-laid structures, but it was found that beating and wet-pressing can help to increase or regain the strength properties, while still preserving the other added functionalities of foam-laid structures (Punton, 1975; Smith & Punton, 1975). The first applications of this foam forming process were in non-wovens, and a pilot scale process was tried for papermaking applications too

in the 1970s, which was not widely applied, and the process was almost forgotten for some decades (Punton, 1975; Smith & Punton, 1975).

2.3 Foam-formed structures

Foam-formed fibre networks have some structural similarities with traditional sheet materials, e.g., paper. Both are connected networks of fibres, but three-dimensional foam-formed fibre networks have some added functionalities compared to the two-dimensional network structure of traditional sheet materials. In water-laid structures, the fibres are oriented in the in-plane direction, and two-dimensional networks are produced. Foam forming allows producing three-dimensional structures in which fibres are oriented also in an out-of-plane direction, Z-direction. (Lehmonen et al., 2020; Punton, 1975; Smith & Punton, 1975)

The fibre network in foam-formed structures has a larger relative bonded area, wider fibre orientation distribution, and large open pores that result in a higher recovery of deformation compared with two-dimensional sheet materials. The fibres in two-dimensional networks are packed more closely, which leads to load-bearing of a small amount of the fibres in the network. The stress buildup is higher towards these fibres under stress or sudden shock, which can result in plastic deformation. (Pauononen et al., 2018)

Foam-formed fibre networks have advantages compared with water-laid two-dimensional fibre networks, e.g., lower density, improved and more even pore size distribution, and wider fibre orientation. Densities less than 100 kg/m^3 can be produced (Figure 5). Foam forming enables also good water drainage properties, which is beneficial in the strengthening of foam-formed structures, since strengthening additives can be used with higher retention levels. This results in higher bulk without tremendous loss in strength properties, which also decreases the cost of raw materials used in foam-formed structures. These value-added structures can be used in a variety of applications in which bulk is a critical asset, including packaging, cushioning, construction, anti-microbial materials in biomedical field, and many other lightweight products. (Kinnunen et al., 2013)

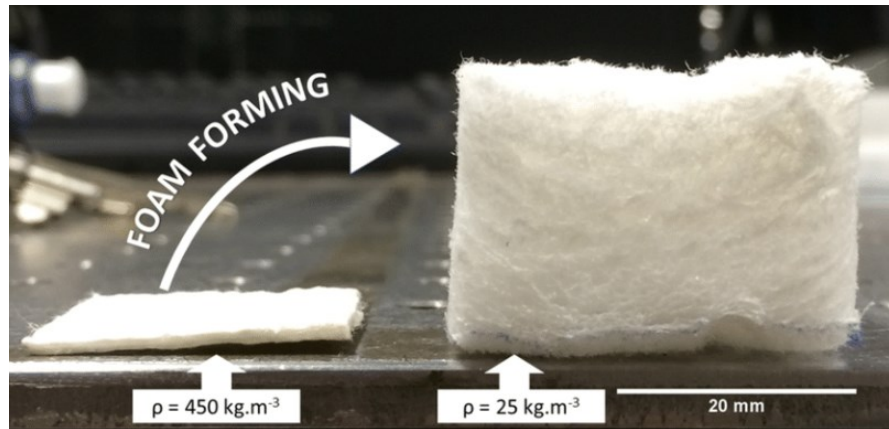


Figure 5. Foam forming technique can result in fibrous structures with low densities.
(Burke et al., 2019)

3 CUSHIONING PROPERTIES

Numerous packages are being transported every day, and during transportation, packages encounter different hazards that the products should survive without deformation or other damages. Thus, it becomes inevitable to protect products from different hazards while transporting the products from production to the final destination, or customers. Cushioning materials become exceedingly important in protecting the product since added cushioning between the product and the outer package absorbs some of the energy that is produced by a sudden shock, which can save the product from substantial damages.

The main purpose of cushioning in packaging solutions is to keep the product protected from sudden shocks, vibrations, and other mechanical stress that the package can encounter during transportation (Department of Defense, 1997). The idea of cushioning is to absorb the kinetic energy through deformation in unexpected shocks, e.g., if the product is accidentally dropped during shipment or transportation.

In addition, to protect package contents when subjected to sudden stress, other purposes of cushioning materials are protecting the product from damages due to extreme variations in climate conditions, such as changes in temperatures, humidity, or sun exposure (Department of Defense, 1997). In many cases, cushioning should protect from

moisture, thus the used materials for cushioning should not be hygroscopic preventing e.g., corrosion or rotting of the inner product (Department of Defense, 1997). Especially when investigating new materials to use in cushioning, production and price for the raw materials should be cost-effective and environmentally compatible to be used on a larger scale.

3.1 Traditional cushioning materials

There are many types of cushioning materials available to be used in packaging, and the two main types of cushioning solutions are blockers and void fillers. Blocking solutions have higher impact resistance, and these cushioning materials can fill some or the entire space between the product and the outer package. Usually, blockers can fill only the edges of the box or product to protect the product from sudden shocks and support fragile parts, e.g., corners and edges of the product (Figure 6). Void fillers fill all space between the product and outer packaging, and the meaning is to stabilize the product in transporting. Typical void fillers are paper, packing peanuts, and air pillows. (Goodwin & Young, 2010)

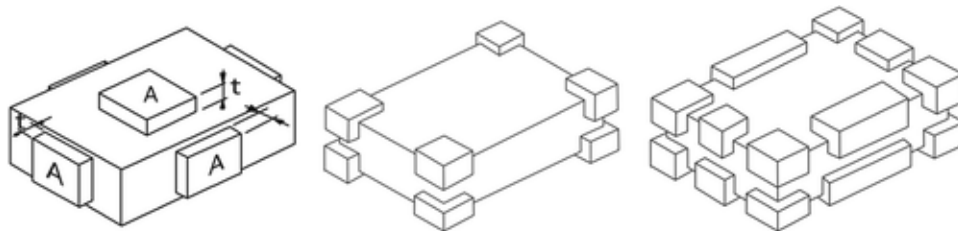


Figure 6. Different types of cushioning blocking solutions stabilizing the product and supporting corners and edges. (Ge, 2019)

Different cushioning materials have different characteristics, and depending on what is being shipped, how much space must be filled, and what kind of functionalities the cushioning needs to have, the best decision to protect products during transport can be chosen (Goodwin & Young, 2010). The most common cushioning materials are polymeric foams, but other polymeric cushioning materials are also available, e.g., bubble wrap

(Dennis, 2011). Polymeric foams are mostly made of polystyrene (PS), polypropylene (PP), polyvinyl chloride (PVC), and polyurethane (PU) (Landrock, 1995). In addition to polymeric cushioning materials, corrugated board and paper wrapping are also widely used alternatives (Dennis, 2011).

3.2 Fragility of packed items

The degree of vulnerability, fragility, can be used to describe the strength when the packaged product is exposed to vibrations or shocks. Fragility can explain the product's mechanical properties, and the product's ability to withstand external forces. Structural damages or functional failures can occur and damage the product when the impact forces acting on the product exceed a certain limit. Fragility can be measured quantitatively, as shown in equation (1):

$$G_c = \frac{a_m}{g} \quad (1)$$

where G_c is the fragility of the product, a_m is the maximum acceleration the product can withstand before damage and g is the acceleration of gravity. A higher G_c value indicates higher strength, i.e., lower damages when facing external forces. (Burgess, 1988)

3.3 Mechanical testing of low-density materials

Many testing methods are available to test the mechanical properties of different materials. There are standardized methods to measure for example tensile strength (EN 1608) and compression strength (EN 826), and the results from these tests are important for foam-formed products that are going to be used in cushioning applications since materials used in cushioning need to protect products from high mechanical stress (Hjelt et al., 2021). It is also important to test the recovery of the deformation after compression (Hjelt et al., 2021).

In this thesis, the focus is on strengthening the foam-formed structures, and the application field is especially in inner packaging or cushioning material and testing of cushioning properties is done with the Platen drop test. The main principle of the Platen drop test is explained below.

3.3.1 Platen drop test

ASTM test procedure, D1596, “Standard Test Method for Dynamic Cushioning Characteristics of Packaging Material” describes a procedure to obtain dynamic shock cushioning characteristics of packaging materials through a drop test (Figure 7) in which a plate with a certain height and weight is dropped on the surface of inspected motionless test sample. The density of a sample is measured before and after the test. In the test, the measured parameters are deceleration (negative acceleration) of the dropped plate, duration of the impulse, and maximum compression of the sample that is determined from the recorded high-speed video from each drop test. These parameters help to determine the essential cushioning properties of foam-formed materials. (ASTM International, 2021)

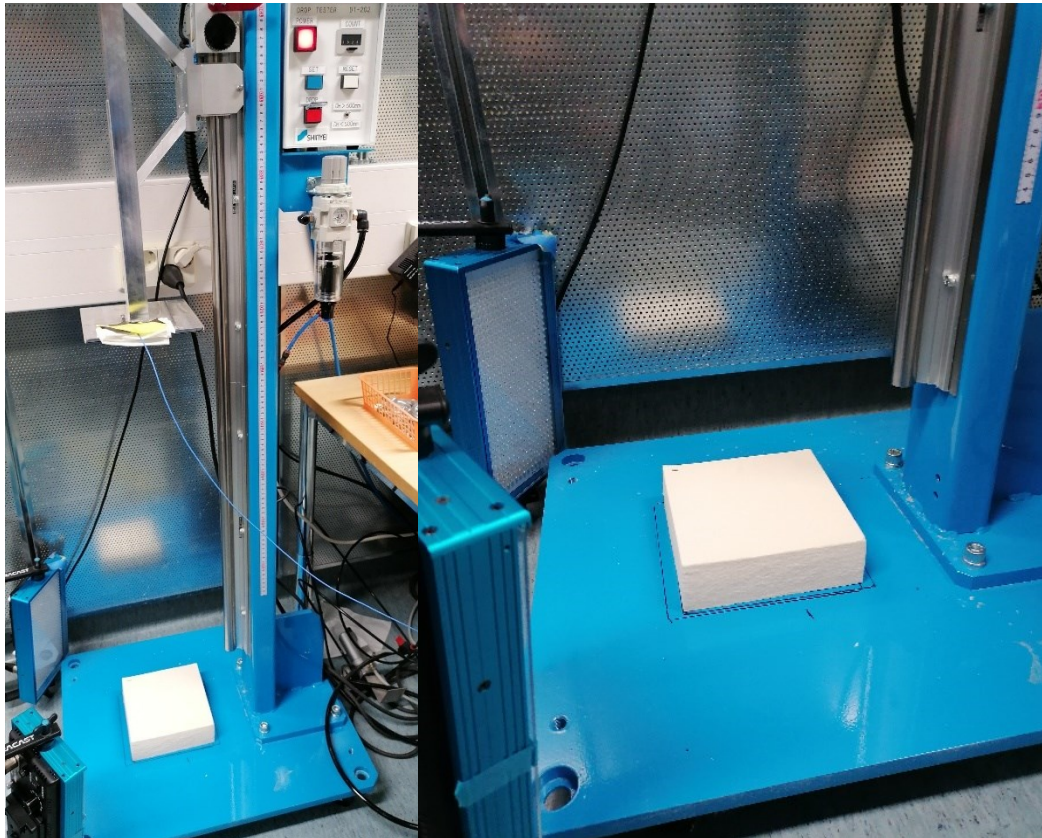


Figure 7. Platen drop tester used to measure strength and resilience of fibrous, low-density structures.

Platen drop test is used to test dynamic compressibility, shock absorption, and recovery (resilience) properties of low-density materials that have application areas in packaging and cushioning. From the obtained results, peak acceleration (a_m) is a key parameter that indicates how well the packaging protects the product during a shock. (ASTM International, 2021)

The time duration of the shock pulse is also an important factor to be taken into consideration. The duration of acceleration-time pulses of sudden shocks usually ranges from 10 to 40 milliseconds, thus it is worth noticing that when packaged systems encounter sudden shocks, e.g., dropping the product, the duration is usually very short (Department of Defense, 1997). The purpose of cushioning is to decrease the maximum deceleration the product faces during the shock (Figure 8).

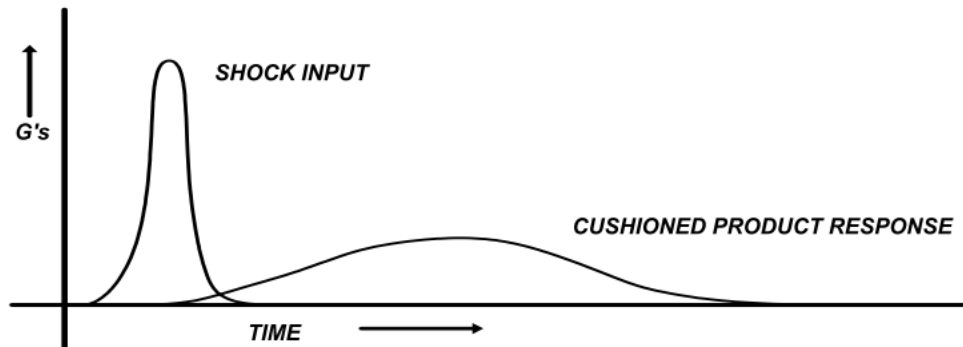


Figure 8. Ideal cushioned product response to shock input. (Mojzes, 2009)

3.3.2 Cushion curve

The obtained results from the Platen drop test are collected into a combined graph, cushion curve (Figure 9). Cushion curves give important information about cushioning materials that can be used when estimating the needed cushioning properties. In the standard test for dynamic shock cushioning properties, the experiment is performed multiple times, i.e., the time to acquire enough data for cushion curves is high. Usually,

this means various sample thicknesses, drop heights, and plate masses, that can increase the total amount of drop tests that are required to over 2000 tests. (Burgess, 1994)

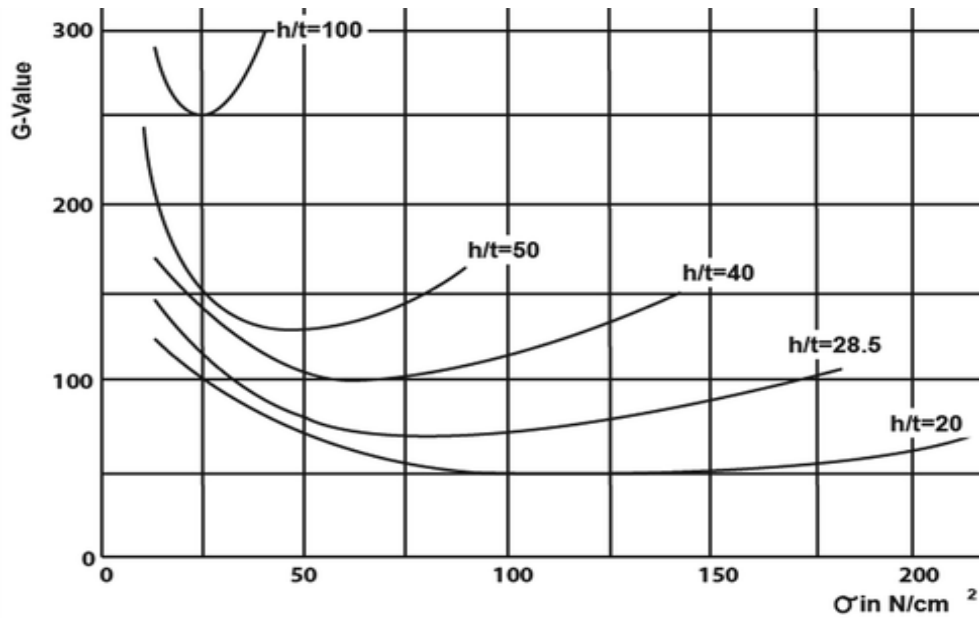


Figure 9. Example of a cushion curve showing G value as a function of static stress. Relationship h/t consists of the drop height, h , and cushion foam thickness, t . (Ge, 2019)

The y-axis of the cushion curve demonstrates the G-value of a sample, which is defined as the ratio of maximum acceleration of the plate during the impact and gravitational acceleration, as shown in equation (1). The x-axis demonstrates the static stress, that is shown in equation (2):

$$\sigma_s = \frac{W}{A} = \frac{mg}{A} \quad (2)$$

where σ_s is the static stress, calculated by dividing the plate weight (W) by the surface area (A) of the test sample. Plate weight can further be calculated by multiplying the mass of the weight (m) with the acceleration of gravity (g). Since the mass of the plate (m) and surface area of the sample (A) are measurement-dependent parameters, using static

stress as a parameter in the cushion curve instead eliminates parameters that are measurement-dependable. (Mojzes, 2009)

When designing the packaging for a product, cushioning curves are applied in the selection of the right cushioning that corresponds to the right packaging parameters. Cushion curves also help in the determination of desired cushioning thickness to provide the right amount of shock absorption and protection to the protected product. (Mojzes, 2009)

Together with G-value or cushion curve, recovery is an important indicator of how much stress the cushioning materials can handle. In the Platen drop test, maximum compression of the sample is determined from the high-speed video that is recorded after the test, and recovery can be measured when the thickness before and after the test is calculated. If recovery of the sample is too low, the breaking distance of the cushioning decreases, resulting in lower absorbance of kinetic energy in sudden shocks, thus cushioning can no longer be functioning the desired way. (Mojzes, 2009)

4 STRENGTH PROPERTIES

Strength is a physical property of a material that resists the deformation of a material under the action of external load or forces. In fibrous materials, strength is a result of multiple factors, including e.g., the type of the fibres that are used and the bonding between the fibres. (Alava & Niskanen, 2006)

One of the main challenges with the properties of foam-formed structures is a decrease in strength compared to the traditional wet web-formed structures. The strength properties of low-density foam-formed sheets can be increased or regained with beating and wet-pressing. However, the problem with wet-pressing and beating is the decrease in bulk, which results in the weakening of some mechanical properties of the final structure, e.g., bending resistance (Lappalainen et al., 2014a; Punton, 1975; Smith et al., 1974). Another option to increase the strength properties of the material is to use strengthening additives and the selection of surfactant can also affect the strength of the material (Lappalainen et al., 2014).

4.1 Factors affecting the strength of foam-formed structures

Strength properties of the foam-formed fibrous structures depend on many factors, but the main factors that affect the strength of the fibrous materials, are defined mainly by the properties of the fibres, for example, fibre length, orientation, stiffness, fibre size distribution, and bonding (Hjelt et al., 2021). Also, refining affects the strength properties, since refined fibres increase the density of the material and increase the number of inter-fibre joints(Hjelt et al., 2021).

Refining can improve the strength of foam-formed structures by increasing internal and external fibrillation of the fibres and generating cellulosic fines. Internal fibrillation refers to the detachment of layers inside the cellulose fibres, i.e., delamination. Delamination occurs by disruption of hydrogen bonding, which increases internal cell wall porosity. Delamination results in better conformability onto uneven surfaces, which improves fibre bonding. External fibrillation occurs, when the microfibrils peel off from the fibre surface, but stay attached onto fibres generating fibrils, that can fit into surface irregularities, thus increasing fibre bonding. (Kang & Paulapuro, 2006; Robinson, 1980)

Burke et al. (2019) have confirmed that by changing the initial liquid fraction the compressive modulus of the fibrous networks can be changed. By changing the initial liquid fraction, the density of the material can be controlled, and when density is increased above the minimum density, the compression modulus increases linearly with increased density (Burke et al., 2019). After a few years, Burke et al. (2021) studied that the previous observations are due to the initial liquid fraction's effect on the fibre orientation and the orientation of the fibres is a more determining factor for the compression strength rather than the size of the voids. The effect is due to a change in foam drainage when varying the liquid fraction since increased foam drainage results in more aligned fibres in the direction of drainage, e.g., z-direction.

Density is one of the most important properties of fibrous structures that determines the mechanical behavior of the structures to a great extent. Density affects the strength of the structure, since density is strongly correlated with the number of contacts between fibres that strengthen the structure. In foam-formed structures in which the density is lower and higher bulk compared to water-laid structures, there is a higher inter-fibre contact area inside the sheets. (Lehmonen et al., 2020; Smith et al., 1974)

The bond strength and inter-fibre contact area are properties that largely affect the strength of fibrous network. In the fibrous network, the fibres are bound together by molecular interactions, and the strength of individual fibres is stronger than fibre-fibre bonds. Thus, the bonds, rather than individual fibres, can be referred to as the “weak link” in fibrous networks. Fibre bonding can be characterized by two main physical parameters, bond strength, and bond area, and many factors affecting bond strength also affect the bond area. In addition, a third parameter, known as the specific load strength, i.e., breaking load per area of bonding, is frequently used in scientific publications as a characterization parameter of fibre bonding. Other variables affect bonding, e.g., internal and external fibrillation, additives, fines content, fibre conformability, and coarseness. (Robinson, 1980)

A higher inter-fibre contact area results in more possible contacts between the fibres, resulting in the stronger network (Ketoja et al., 2019). The number of inter-fibre bonds depends on the density of the fibrous structure, but in addition fibre orientation and geometry affect bonding too (Ketoja et al., 2019). Due to the difficulty of determining the number of bonds experimentally, a variety of models have been proposed. The models that have been used for fibrous 2D networks, cannot be applied to 3D networks, since in general, the fibres in 3D fibrous structures are not aligned in-plane direction (Ketoja et al., 2019). Models to estimate the contact count in 3D networks have been developed, e.g., Komori & Makishima, 1977 have introduced a model to calculate the number of fibre-fibre contacts for random fibre distributions, that can be applied to 3D fibrous networks, per unit volume.

4.2 Factors affecting compression recovery

Fibre network in three-dimensional (3D) foam-formed structures displays higher deformation recovery compared to two-dimensional papers and sheets as foam forming utilizes multi-scale structural features that can enhance the elasticity of the produced materials under compression. Elasticity can be improved e.g., by the addition of polymers that can gather into fibre joints, helping the fibrous structure to recover after compression without major deformation in the structure. (Paunonen et al., 2018)

Compression recovery of foam-formed structures highly depends on how well the fibre segments can handle load under stress. Many earlier theoretical ideas on how the three-dimensional fibrous networks work under compression, consider deformation to take place through continuous local deformations, e.g., bending of individual fibres (Beil & Roberts Jr, 2002; van Wyk, 1946). Ketoja et al. (2019) have stated some problems regarding these earlier theoretical models: if the principal deformation model is assumed to be bending of fibres, the compression strength of the structure should act like density to the cubic power, but it has been noticed, that the power is generally lower, close to 2, excluding this idea. Also, Ketoja et al. (2019) inspected that a high amount of stress is released by sudden discontinuous movements of individual fibres, and proposed, that a significant amount of stress release comes from the buckling of fibres instead of bending of fibres. Buckling of fibres can occur even though the orientation of the fibres would not be in line with the compression direction, since under vertical compression, the stress is directed also to transverse directions that is due to Poisson effect (Ketoja et al., 2019; Sotoodeh, 2021). Poisson effect explains that when material is being stretched, the structure expands also in the direction that is perpendicular to the compression (Ketoja et al., 2019; Sotoodeh, 2021).

Together with the buckling of fibres, bond failures or opening is also another type of local deformation mechanism that can result in local stress release and eventually cause the network structure to collapse over time. It is worth noticing that buckling of fibres can occur without bond failures, and it is still under research, which mechanism affects the most recovery of fibrous structures. (Ketoja et al., 2019)

5 ADDITIVES TO IMPROVE STRENGTH PROPERTIES

In this chapter, some possible alternatives to use as additives in the foam forming process are introduced. Use of some of the additives mentioned in this chapter have been tested before in the foam forming process, e.g., cellulose nanofibrils (CNF), polyvinyl alcohol (PVA), cationic starch, and chitosan (Hou & Wang, 2017; Lappalainen et al., 2014b; Paunonen et al., 2018; Torvinen & Lahtinen, 2015, Wu et al., 2022). Additives are important in the papermaking industry to improve the wet and dry strength of the paper

(Neimo, 1999). High wet strength is important especially for e.g., tissue paper, filter paper, and liquid packaging board applications (Neimo, 1999). Dry strength properties are important for all paper and board applications and are under research in this thesis.

Many commonly used strength-improving additives are hydrophilic polysaccharides or polymers that can form hydrogen bonds with cellulosic fibres (Fornué et al., 2011; Liu et al., 2017). In the traditional papermaking process, a mass fraction of 0.1-0.35% is usually enough to improve the strength properties of the materials (Liu et al., 2017). Too high content of additives usually reduces the strength properties due to the lower density of a fibre network, strength of bonds, and relative bonded area (Scott 1987, Lappalainen et al., 2014). In addition, one challenge with some additives is poor mechanical retention of the additives, which can be improved with retention aids.

The strength properties of foam-formed structures can be improved with a variety of fibrillar and polymeric materials and fines. The strength-improving mechanisms are connected to increased bond strength and total inter-fibre contact area. The addition of fines can increase the number of bonds by building “bridges” between fibres. The build-up of bridges drags fibres in contact with other fibres increasing the number of bonds. Using fibrillar and polymeric additives also affects the strength of individual bonds by forming a larger contact area and increasing the entanglement of fibrils between fibres, or inter-fibre fibrils. (Pöhler et al., 2020; Schmied et al., 2012)

Many additive polymers can increase the dry strength of the material and improve bond strength by interacting with fibres in different ways. The interactions can be categorized as covalent bonding, ionic attraction, hydrogen bonding, and van der Waals forces (Hamzeh et al., 2013). Many commonly known strength-increasing additives, such as starches, interact with fibres forming hydrogen bonds between fibres increasing the amount of lower energy bonds (Hamzeh et al., 2013).

5.1 Cellulose nanofibrils (CNF)

Cellulose nanofibrils (CNF) are structural units of cellulosic fibres with a size less than 100 nm at least in one dimension. CNF is produced by isolating cellulosic fibres with mechanical fibrillation. CNF has a high aspect ratio, the length being up to a few

micrometers and diameter of 5-50 nanometers, and high mechanical stiffness. CNF forms easily hydrogels in aqueous solutions. (Ferreira et al., 2020)

CNF is a potential additive to use as a strength-enhancing additive since the surface of CNF is rich with hydroxyl groups, and when added into the pulp, the hydroxyl groups on the surface can form hydrogen bonds with pulp fibres increasing the strength of the fibre network (Figure 10). The reinforcement mechanism of added CNF can be explained by increased surface area when CNF fills the voids and pores inside the fibre network but also by increased fibre-to-fibre contacts at the molecular level. It has been studied that if CNF is used together with some cationic polymers, e.g., polyamine epichlorohydrin (PAE), the wet and dry strength can be improved even more. (A. Li et al., 2021)

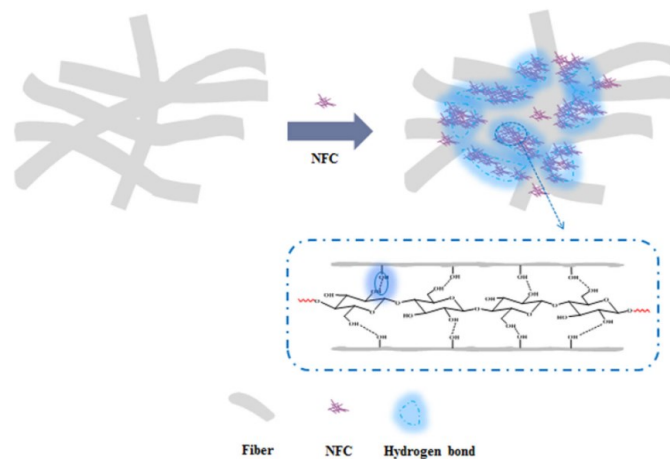


Figure 10. Cellulose nanofibres, or nanofibrillated cellulose (NFC), enhance the strength of pulp fibres by formation of hydrogen bonds. (A. Li et al., 2021)

5.2 Polyvinyl alcohol (PVA)

Polyvinyl alcohol (PVA) has been widely used in papermaking as a dry-strength agent for example in printing and packaging papers. PVA is a linear and synthetic water-soluble polymer that is produced by hydrolyzing polyvinyl acetate (PVAc) with sodium hydroxide (NaOH) and methanol (CH₃OH). PVA can be used as a nonionic tensid, if not all acetate groups are hydrolyzed to hydroxyl groups, and since the molecule contains both,

hydrophilic and hydrophobic groups, PVA can also be used as a surface-active agent. (Amann & Minge, 2011)

PVA stabilizes the foam by decreasing the surface tension between gas and liquid phases. Acetate groups are hydrophobic and are in contact with air bubbles, and hydroxyl groups are hydrophilic and in contact with the continuous liquid phase. The foam formation of PVA depends on the ratio of hydrophobic and hydrophilic groups. The strengthening effect of PVA is based on crosslinking inter-fibre bonds, but also the opening of large voids in the microporous structure. (Amann & Minge, 2011; Hjelt et al., 2021)

5.3 Guar gum

Guar gum is a natural polysaccharide that is derived from the seeds of the Indian Tree. Guar gum has a linear backbone consisting of mannose and galactose in a ratio of about 1.6-1.8:1 (Figure 11). Guar gum is a hydrophilic polymer that has a high molecular weight, and it can be easily modified, e.g., cationic guar gum is a modified polymer that has been used in cosmetics as an emulsifier. Guar gum has been widely used in other application areas as well, such as in the food, pharmaceuticals, and papermaking industry. (Mudgil et al., 2014; Strand et al., 2019)

The addition of guar gum to foam-formed structures can increase strength by hydrogen bonding activity of guar gum since hydroxyl groups of guar gum can form hydrogen bonding with cellulosic material. (Mudgil et al., 2014)

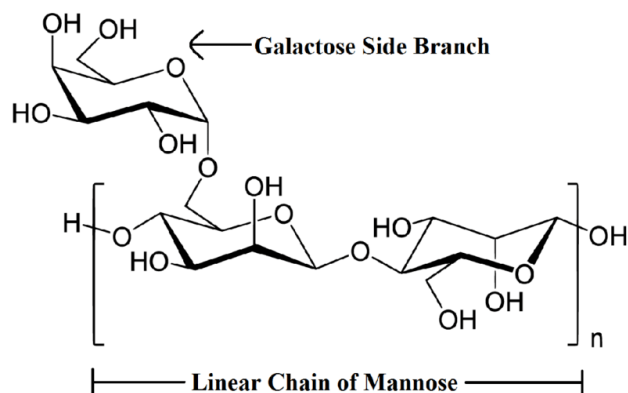


Figure 11. Chemical structure of guar gum showing linear chain of mannose and side branch of galactose. (Pandya, 2013)

5.4 Carrageenan

Carrageenan is a sulphated polysaccharide that is extracted from a natural origin, various species of red seaweeds (Rhodophyta). The structure of the carrageenan is similar to pectins in land plants. Carrageenan is a high molecular-weight polymer, the average relative molecular mass being over 100 kD. The backbone of carrageenan consists of alternating units of 3,6-anhydrogalactose and galactose, and the units are connected by β -1,4 and α -1,3 glycosidic bonds (Figure 12). Carrageenan is anionic and hydrophilic due to sulphated monosaccharides in carrageenan, and approximately 15-40% of carrageenan's monosaccharides are sulphated. (Liu et al., 2017) Carrageenans are categorized into three classes based on the number of sulfate groups per disaccharide unit. Kappa-carrageenan has one, iota-carrageenan has two, and lambda-carrageenan has three sulfate groups per disaccharide unit. (Zia et al., 2017)

The use of seaweed as a source of materials has been under research in recent years. As a widely abundant, environmentally friendly, and fast-growing feedstock, the use of seaweed could help in meeting the needs for sustainable material alternatives. As carrageenan is extracted from marine algae, and aquatic biomass, using carrageenan would not cause land use or food-vs-fuel conflicts that are commonly an issue with conventional sources of cellulose. (Liu et al., 2017)

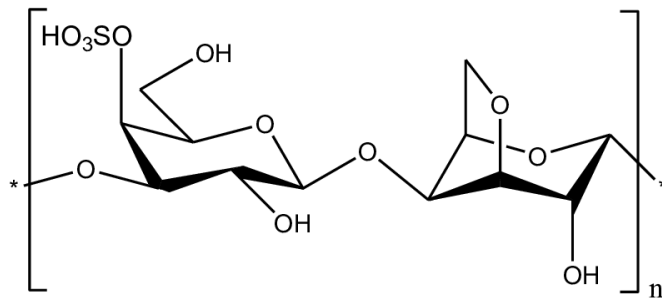


Figure 12. Chemical structure of kappa-carrageenan has one sulfate group per disaccharide unit. (Solov'eva et al., 2013)

Carrageenan has been used in various applications before, and one of the most common commercial applications has been in the food industry, especially as a thickening, or stabilizing agent. Carrageenan has also been used in cosmetics and medicine. Since the structure of carrageenan is similar to many other widely used natural high-molecular-weight polymers, carrageenan could be a viable alternative to use instead of e.g., other gums. Reinforcement mechanism of carrageenan is based on forming of hydrogen bonds between the hydroxyl and sulfate groups of carrageenan with hydroxyl groups of cellulose fibres. (Liu et al., 2017)

5.5 Agar

Agar is a heterogeneous mixture of polysaccharides. Agar is extracted from a few species of red seaweeds, *Gelidium* and *Gracilaria*. Agar is a polymer with a high average molecular weight that varies from 80,000 to 140,000 depending on the origin and extraction technique. The backbone of agar is composed of alternating β -1,3- and α -1,4-linked galactose units (Figure 13). These polysaccharides can form two different structures: agarose is a linear polymer with a neutral charge, and agaropectin is a sulphated polymer with an anionic charge that has a lower degree of polymerization (DP) compared to agarose. (Vishtal & Retulainen, 2014)

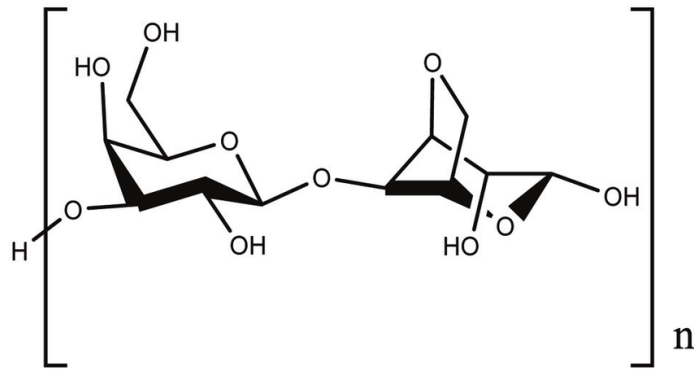


Figure 13. Backbone of agar consists of B-1,3-linked and a-1,4-linked galactose units. (Rahman, 2018)

The structure of agar has similarities with cellulose, which predicts the suitability to use of agar in the mixture with cellulose. The use of agar as a strength-improving agent has been studied in two-dimensional papers. The reinforcement effect of agar is based on strengthening the fibre-fibre bonds by the addition of hydrogen bonds and creating a more uniform fibre distribution, which results in more even stress distribution in the fibre network. It is worth noticing that the penetration of agar through the fibrous network can be limited due to the high gel formation of agar on the surface of the papers. In one of the previous studies, the agar was added by spray addition on the two-dimensional paper surface, and the gel layer formed a film upon drying. (Vishtal & Retulainen, 2014)

5.6 Cationic starch

Cationic starches are one of the most common chemicals used commercially in papermaking to increase the dry strength of the material. Since cellulose fibres have a slightly anionic charge, cationic starch was developed to improve retention and the efficiency of starch utilization on fibres in papermaking, promoting adsorption on the fibre surface by electrostatic attraction. (Hamzeh et al., 2013; Malton et al., 1998)

Starch has a sufficient molecular size to span inter-fibre distances, as well as a tendency to form hydrogen bonds with cellulosic materials. Cationic starch can be used as a retention aid together with other additives, e.g., anionic fibres or polymers, increasing the

retention rate of the additives that are mixed with fibres, water, and surfactant in foam forming. (Hamzeh et al., 2013)

5.7 Chitosan

Chitosan is the second most widespread natural polysaccharide, and it is formed by deacetylation when chitin reacts with an aqueous hydroxide solution (H. Li, Du, Xu, et al., 2004). The structure of chitosan is similar to cellulose, but in chitosan one of the hydroxyl groups is replaced with an amino group (Figure 14). Because of these amino groups in the primary structure of chitosan, chitosan is acid-soluble, but insoluble in water under alkaline conditions. (Laleg & Pikulik, 1993).

In papermaking, chitosan has been investigated widely, and it can be used for many purposes, e.g., dry and wet strength agents, sizing, coating, retention, and antibacterial agent (Kjellgren et al., 2006; Laleg & Pikulik, 1991, 1993; H. Li, Du, & Xu, 2004; H. Li, Du, Xu, et al., 2004). Chitosan can improve the strength properties of fibrous structures by creating stronger inter-fibre bonding. When interacting with fibres in the presence of water, the amino groups in the primary structure of chitosan come into contact with cellulose fibres, and ionic and imino bonds can form between chitosan and pulp fibres. (Hamzeh et al., 2013)

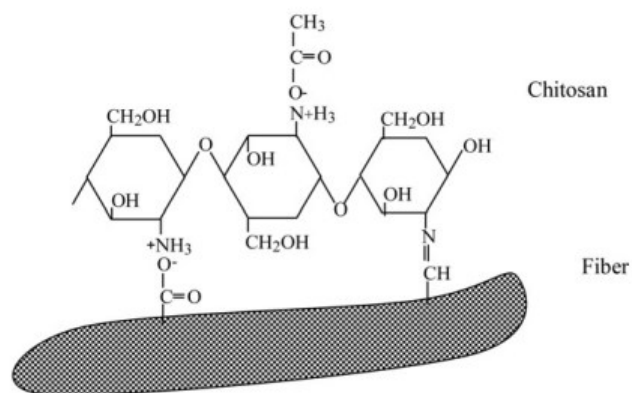


Figure 14. Primary structure of chitosan contains amino groups that can form ionic and imino bonds with hydroxyl groups of pulp fibres. (Hamzeh et al., 2013)

5.8 Natural rubber

Natural rubber is a biobased polymer that can be harvested from rubber trees and is composed of cis-1,4-polyisoprene units. It is one of the most widely used polymers, used especially for tires. Natural rubber is also used in many other applications, e.g., medical devices, balloons, rubber boots, and the construction industry. The natural rubber has unique characteristics especially in stress-strain behavior, as it is elastic and can be stretched under an external force and can revert to its original shape. This elastic behavior of natural rubber works in a narrow range of temperatures, and when the temperature is raised over a suitable range, the structure becomes sticky, and below the suitable temperature the structure becomes brittle, and the elastic behavior disappears. By vulcanization, some properties of natural rubber can be improved. Vulcanization occurs by heating natural rubber molecules with vulcanizing agents, crosslinking the structure, and resulting in a three-dimensional network, that has improved mechanical properties. (Kumagai et al., 2019)

Natural rubber can be used as a reinforcing element in foam-formed fibrous structures since natural rubber can form bonds with the surface of cellulose (Flink et al., 1988). Since natural rubber is hydrophobic and non-polar, the formation of aqueous foam offers a natural carrier for natural rubber molecules to become attached to the air bubbles, resulting in stronger adhesion to the structure. (Paunonen et al., 2018)

5.9 Crosslinkers

Crosslinking reagents, or crosslinkers, are molecules that can form covalent bonds between two or more molecules through intermolecular or intramolecular bonding. Crosslinkers contain at least two reactive ends or groups capable of reacting with certain functional groups on other molecules, creating new bonds. Crosslinking is a chemical reaction, that can be initiated by heat, irradiation, pressure, or a change in pH. As an example, vulcanization is cross-linking that utilizes heat to change the chemical structure of some materials. As mentioned before, vulcanization is commonly used to change natural rubber to harder, durable material, and this technique is widely used for many applications, e.g., tires. (Zweifel et al., 2009)

5.10 Retention aids

Retention aids are usually high molecular weight, water-soluble polymers that are added into the mass, or cellulosic fibre slurry, to improve the retention of fine particles, e.g., fillers or other additives. Using retention aids is not only improving certain properties of the structure but also helps in achieving an environmentally responsible process, since using retention aids helps the additives to stay in the produced material, not draining away with the excess water to be removed during the wastewater treatment process. Retention aids can also promote dewatering, thus saving energy in the process. In the papermaking process, retention aids also allow an increase in the production rate. This can be explained by the increased speed in water removal from the wet web, which is one of the main factors affecting the maximum rate of production. A few of the most used retention aid polymers are cationic and anionic acrylamide copolymers (cPAM, aPAM) and polyethylene oxide (PEO). The dosage of retention aid that is enough to achieve a certain level of retention efficiency, can be expected to increase with higher specific surface area of the additives used, e.g., smaller particles. (Hubbe et al., 2009)

In the foam forming process, retention aids can help various strengthening agents to retain in the structure. This can be noticed especially with chemically unstable additives, and even though the additives would have higher affinities towards cellulosic fibres, some parts of the additives can adsorb onto the fines and not the fibres, which results in decreased retention efficiency, and help of retention aids is needed.

6 CHARACTERIZATION METHODS

To develop foam-formed structures, it is important to understand and characterize the structural properties of the produced materials. There are some challenges in the characterization of porous foam-formed structures, such as wide pore size distribution, variation in the orientation of the fibres, and low density (Hjelt et al., 2021). Low density makes it more difficult to recognize the borders of the individual pores or a sample (Hjelt et al., 2021). Regardless of these challenges, the existing characterization methods are competent to obtain structural properties of foam-formed materials.

6.1 Micro-computed X-ray tomography (μ XRT)

X-ray microtomography is a quantitative and non-destructive method that uses X-rays to create cross-sections of the internal structure of samples that can be rendered into three-dimensional high-resolution images in the range of 1-100 μm (Adams & Barbante, 2015; Lecourt et al., 2018; Paunonen et al., 2018). Micro-computed X-ray tomography can be used to obtain 3D models of even fragile materials since the method does not destruct the samples (Adams & Barbante, 2015; Lecourt et al., 2018). The principle of μ XRT technique is to stack 2D images that are captured from x-ray absorption of the rotating sample, and 3D images are reconstructed computationally from the captured 2D images (Landis & Keane, 2010; O'Sullivan et al., 2018). The X-ray tomography can be used to explain fibre orientations in foam-formed structures, and to quantify the internal structures of the fibre networks (Burke et al., 2021; Pöhler et al., 2020; Paunonen et al., 2018).

6.2 SEM Imaging

Scanning electron microscopy (SEM) is a characterization method that can be utilized to surface imaging of fibre networks. Compared to traditional microscopes, SEM provides higher resolution, and a lot of specimens can be in focus at the same time. SEM uses a beam of electrons that are produced in the electron gun, and the beam is focused on the sample. When the beam encounters the sample, electrons are backscattered, and detectors convert these into a signal that hit the screen, resulting in the final image of the sample. Since SEM is done under vacuum conditions, moisture is needed to be removed from the characterized samples before imaging to prevent evaporation of water in the vacuum. Also, when imaging non-conductive materials, the sample must be lightly coated with a conductive material, or a low vacuum should be used. (McMullan, 2006)

In the characterization of foam-formed structures, results from SEM imaging can give information about the surface topography, for instance, the roughness of the surface, the composition of the sample, and the distribution of chemicals.

7 ENVIRONMENTAL ASPECTS

In the invention of new alternatives for packaging solutions, the focus in research has lately been strongly on environmentally friendly materials, e.g., biodegradable, recyclable, recycled, and reusable materials. Currently, the most used cushioning materials are based on non-renewable resources, are not biodegradable, and can be difficult to recycle. Legislations related to materials to be used are getting stricter, and manufacturers and brands must start looking for other alternatives, that fulfil the new rules. Selection of materials can be challenging for brands, and consumers can get confused about what is the “right” option to choose. Especially nowadays when brands know that being environmentally friendly affects sales positively, some brands can use bio-based materials that seem environmentally friendly and ecological, but these materials can still face the same problems as some fossil fuel -based materials.

In foam-formed materials, cellulose fibres are the base material for the whole structure. Cellulose is a highly potential alternative to use also in other bio-based applications. Cellulose fibres have many advantages compared to using some other alternatives, such as bio-based origin, biodegradability, recyclability, low cost, low density, stiffness and strength, and high availability (Venkatarajan & Athijayamani, 2021). In addition, the type of chemicals used to increase the mechanical performance of foam-formed structures is also an important factor to investigate beforehand to ensure that the material is a recyclable or otherwise environmentally friendly alternative to use instead of traditional petrochemical-based plastics.

Together with the materials used for cushioning materials, the amount of packaging material to be used is also an important factor regarding sustainability considerations. A certain amount of packaging and cushioning materials is needed to protect the inner product, and the amounts can be estimated with cushion curves, but in some cases, over-packaging can be seen as an issue, leading to high amounts of unnecessary waste. Some manufacturers and brands have chosen to use oversized outer packaging for their products, increasing the amount of inner cushioning to immobilize the product inside the package (Dennis, 2011). If reduction of packaging materials is not a preferable option, choosing more environmentally responsible materials or processes can be a solution.

EXPERIMENTAL PART

In this chapter, the materials and methods for experiments are explained together with the main results. The main purpose of the experiments was to investigate the effects of the addition of different amounts of additives on the strength and resilience of foam-formed fibrous structures. Experiments took place at VTT Technical Research Centre of Finland, Jyväskylä, Finland. The porous samples were prepared using a large sheet mold, and testing of cushioning properties was done with the Platen drop test. The results after drop tests were interpreted, and two characterization methods, micro-computed X-ray tomography, and SEM imaging were used.

8 MATERIALS

In all prepared samples, spruce bleached chemi-thermomechanical pulp, (B)CTMP was applied. (B)CTMP was obtained from a Swedish pulp mill (Rottneros AB, Rottneros Mill, Sweden). A non-ionic alkyl polyglucoside, AG6210 (Nouryon) was used as a foaming agent. The foaming agent was utilized to foam the fibre-water suspensions with an amount of 1.6 g/l.

The selection of chemicals to improve strength properties was based on previous studies. In the studies, the chemicals had increased strength either in traditional papermaking or foam forming. Eight different chemicals were used in one, two, or three addition levels. Citric acid was utilized as a crosslinker in one sampling point with chitosan and one reference sample. Cationic starch was used as a retention aid with some of the anionic sampling points including HefCel (high-consistency enzymatically fibrillated nanocellulose), k-carrageenan, and anionic guar gum. The dosage of used chemicals was based on previous studies, viscosity, and usability of chemicals.

High-consistency enzymatically fibrillated nanocellulose, HefCel, was acquired from VTT Espoo. HefCel solution was prepared by creating a 4% suspension in distilled water. The suspension was disintegrated using a dispergator (Netzsch ShearMaster) and mixed for approximately 30 minutes at 3000 rpm. HefCel solution was added in three different addition levels: 5%, 12.5%, and 20%.

Three different guar gum grades were obtained from Polygal: Non-ionic high-viscous guar gum (Polygym 26/1-75), non-ionic low-viscous guar gum (Polygym 240/05), and anionic guar gum (Polycol M-204). 1 wt.% guar gum solutions were prepared with a mixer (Silverson L5M-A) at 5000 rpm, and depending on the molecular weight, mixing time varied from 10 to 30 minutes from low to high molecular weight polymers. The viscosities for 1 wt.% guar gum solutions were obtained with a rheometer (Brookfield Viscometer DV-11+ Pro EXTRA, AMETEK Brookfield, Middleboro, MA, USA). The measured viscosities for guar gum solutions were approximately 5000 mPa·s, 70 mPa·s, and 1000 mPa·s, respectively. Guar gum solutions were added in two different addition levels: 0.5% and 5%.

K-carrageenan (Thermo Fisher Scientific) solution (2 wt.%) was prepared with a mixer, and the measured viscosity for k-carrageenan solution was approximately 50 mPa·s right after mixing. The viscosity increased remarkably after cooling down the solution, and the structure of the solution changed from viscous liquid into rigid gel. K-carrageenan was added in two different addition levels: 0.5%, and 5%, and also with and without cationic starch resulting in four different sampling points.

1 wt. % chitosan solution (high molecular weight, Sigma Aldrich) was prepared by dissolving chitosan in aqueous solution of acetic acid (0.1 M). Chitosan was used with two different addition levels, 0.5% and 5%, and also one sampling point was prepared with 5% of chitosan and 4% citric acid resulting in three different sampling points. Two types of synthetic latex were acquired from CH Polymers (CHP557), and from Trinseo (HPH23), and they were used with an addition level of 20%. Citric acid (Sigma Aldrich) solution (1 wt.%) was used as a crosslinker in some trial points, and cationic starch (Raisamyl 50021, Chemigate) was used as a 5 wt.% solution as a retention aid in some of the samples. The composition of the prepared samples is listed in Table 1.

In addition to CTMP samples, also ready-made EPS (Bewi) and PU (producer unknown) were used as references to compare the results of strength and resilience with petroleum-based alternatives. EPS reference was the same size as other samples, but PU reference was made from four 15 mm thick plates that were piled up to result in 60 mm thick sample. The drop height for PU reference was adjusted 10 mm higher in order to keep the drop height the same with the other samples.

Table 1. Composition of the samples. In addition, all samples included 568 g dry CTMP pulp (4% suspension), 1.6 g/l foaming agent AG6210, and water until the initial volume before generating the foam was 16 liters.

ID	Additive	Addition of additive (%)	Addition of citric acid (%)	Addition of cationic starch (%)
A1	-	-	-	-
A2	-	-	-	-
A3	-	-	-	1
A4	-	-	4	-
SL1	CHP557 Synthetic latex	20	-	-
SL2	HPH23 Synthetic latex	20	-	-
HC1	HefCel	5	-	1
HC2	HefCel	12.5	-	1
HC3	HefCel	20	-	1
KC1	K-carrageenan	0.5	-	-
KC2	K-carrageenan	5	-	-
KC3	K-carrageenan	0.5	-	1
KC4	K-carrageenan	5	-	1
C1	Chitosan	0.5	-	-
C2	Chitosan	5	-	-
C3	Chitosan	5	4	-
G1	Polygum 26/1- 75 Guar gum	0.5	-	-
G2	Polygum 26/1- 75 Guar gum	5	-	-
G3	Polygum 240/05 Guar gum	0.5	-	-
G4	Polygum 240/05 Guar gum	5	-	-
G5	Polycol M-204 Guar gum	0.5	-	-
G6	Polycol M-204 Guar gum	5	-	-
G7	Polycol M-204 Guar gum	0.5	-	1
G8	Polycol M-204 Guar gum	5	-	1

9 METHODS

9.1 Sample preparation

All samples (Table 1) were prepared using CTMP fibres, and surfactant, AG6210, and the variables were type and amount of additives, use of retention aid (cationic starch) and crosslinker (citric acid). Samples were prepared using approximately 4% consistency (B)CTMP fibres.

The foam-formed samples were prepared with a laboratory sheet mold at VTT Jyväskylä (Figure 15). The foams were generated by mixing the pulp dose, foaming agent, additives, and water in a 40 L mixing tank so that the initial volume was 16 liters. The tank was cylindrical with four disk-style impellers. Mixing was done with at a rotational speed of 3000 rpm. When the foam reached the highest impeller, mixing was continued for 5 minutes. The foaming time varied between 11 minutes to 22 minutes for different samples (See Appendix A). The final volume of foams was 42 liters, so the target was to reach an air content of 60% after foaming. After mixing, the wet foam was poured into a rectangular sheet mold (Figure 15) with an area of 0.1828 m² (43 cm x 43 cm) along a tilted plate to orientate the fibres slightly. A forming mesh was added on the top of the sample, and it was pressed slightly to obtain more even surface. The foam was left in the mold for 1-2 hours until no high water drainage was seen under the mold. The samples were dried at +70°C oven overnight (24 hours).



Figure 15. A foaming tank used to prepare the fibre foam (left). Foam poured along a tilted plate into a rectangular sheet mold (right).

After drying, the sheets were re-wetted to 50% dry matter content with a compressed air paint sprayer (Figure 16) and the sheets were placed into plastic bags for 4 hours. After re-wetting, the samples were pressed between two metal plates with spacers in the corners to thickness of 51 mm to adjust the density on the desired level. The pressing was done with a hydraulic laboratory sheet press designed by VTT and dried overnight (24 hours) at +70°C oven with weight on metal plates (Figure 16).



Figure 16. Dry sample was re-wetted into 50% dry matter content (left). After re-wetting, the samples were pressed into desired thickness with a dynamic press and were dried overnight in the oven (right).

Pressed and dried samples were trimmed and cut with a bandsaw (Makita LB1200F) into four test pieces of size 180 mm x 180 mm (height 51 mm) (Figure 17). The final samples were left at standard test conditions ($23^{\circ}\text{C} \pm 2^{\circ}\text{C}$, $\text{RH } 50\% \pm 4\%$) at least for 4 hours before mechanical testing was done with the drop tester.



Figure 17. The samples were cut into four pieces of size 18 cm x 18 cm and left in standard test conditions (23°C RH 50%) for 4 hours before drop tests.

Basis weight of the samples was measured after balancing samples at standard test conditions. Thickness of the samples was measured with a laser beam before further tests.

9.2 Sample testing

Mechanical testing, a dynamic shock cushioning test, was done with the Platen drop test. For each trial point, three parallel samples were tested with three drops in a row. The specimens with the desired thickness (about 2" = 5.08 cm) and length and width (18 cm x 18 cm), were placed in a testing area (modified Drop Tester DT-202, Shinyei Technology), and the plate with a mass of 3.53 kg was dropped from a drop height of 84.5 cm (33.26"). The time evolution of acceleration, or deceleration, of the plate, was measured with an accelerometer, and data acquisition system (Lansmont TP3 Lite) was used to collect data. Each drop was captured to a video with a high-speed camera (Y3, IDT, Tallahassee, FL, USA). Together with deceleration, other parameters that were captured after each drop, were maximum displacement of the sample (mm), strain (%), and resilience (%), which can be explained with equations (3) and (4):

$$\text{strain (\%)} = \frac{\text{maximum displacement (mm)}}{\text{initial thickness (mm)}} \quad (3)$$

in which maximum displacement (mm) was measured from the obtained video from high-speed camera, and initial thickness (mm) was measured with a caliper before drop tests.

$$\text{resilience (\%)} = \frac{\text{final thickness (mm)}}{\text{initial thickness (mm)}} \quad (4)$$

in which the final thickness was measured with the caliper after every drop.

9.3 Sample characterization

Micro-computed X-ray tomography (XuCT) (1172, Skyscan/Bruker, Kontich, Belgium) was used to examine the internal structure of some selected samples. A tomographic scanner was used with a tube voltage of 40 kV and a current of 300 μ A. Samples that were imaged with a tomographic scanner, were further imaged with SEM imaging to obtain high-resolution images of the internal structure of the samples. The dry fibre samples were sputtered with a 5 nm layer of Au/Pd with a sputter coater (Leica EM

ACE200) before SEM imaging. A field-emission scanning electron microscope (FE-SEM Merlin, Carl Zeiss Microscop, Oberkochen, Germany) was used with an acceleration voltage of 2 kV and a current of 60 pA. SEM images were obtained with magnifications of 100 and 1000 times of original magnification.

10 RESULTS

10.1 Foaming and sample structure

Foaming time varied from 11 to 22 minutes between the samples (see Appendix A). The fastest foaming time was observed with samples that included high-molecular weight chemicals; high-molecular weight guar gum and carrageenan, and the longest foaming time was observed with samples including chitosan in the structure. Trial points which included chemicals that easily form gels in aqueous environments, e.g., guar gum, k-carrageenan, and HefCel, drained water relatively slow at room temperature, keeping the moisture inside the foamy structure. Those samples were dried for 36-48 hours at 70°C, whereas other samples were dried for 24 hours at 70°C until the sample was observed to be dry. Preparation of some of the samples was more difficult, e.g., it was noticed that samples with higher chitosan content (5%) were tightly attached to the mold after drying, and it was more challenging to take the sample out of the mold without causing breakage of the sample. The additive that had the highest viscosity of all chemicals used, k-carrageenan, had to be mixed almost immediately with pulp dose, surfactant, and water after preparation of the solution or heating it. This was made to avoid k-carrageenan solution turning to a rigid gel that was seen when cooled down close to a room temperature.

The structure varied between the samples, and some of the samples which included chemicals that easily form gels in aqueous solutions, e.g., k-carrageenan and guar gum, especially with higher contents (5%), were observed to have more soft structure, whereas samples with chitosan and synthetic latex were the most rigid out of all samples.

10.2 Drop test results – Strength and resilience

The density of the samples varied from 58 kg/m³ to 75 kg/m³, and some correlation was expected between density and maximum G values – the assumption was that the higher the density of samples, the higher the maximum G value and resilience of samples. The results after the first drop are presented in Figure 18, which presents the average of three parallel first drops with standard deviation. The corresponding sample ID's and sample compositions are listed in Table 1. It is noticed that values of maximum G in the Z-direction do not change drastically between the samples when the density increases, rather the type and amount of chemicals in the samples is a determining factor.

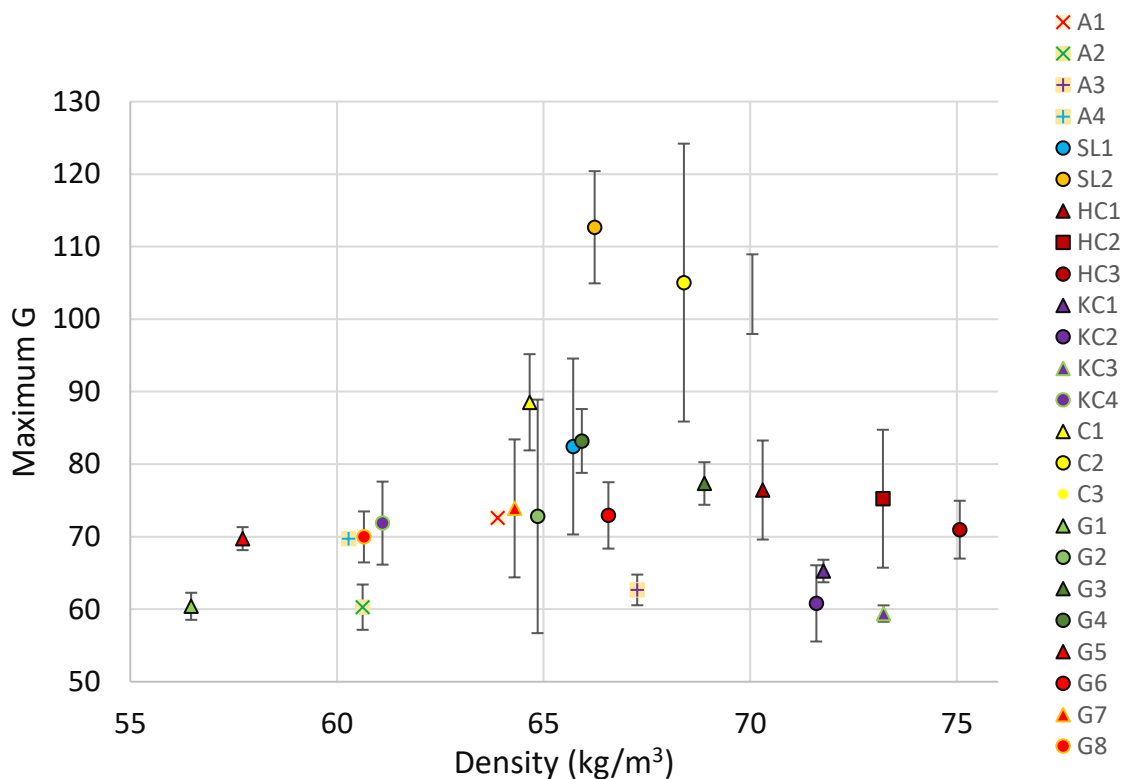


Figure 18. Maximum G values after the first drop in drop tests. Samples SL2, C2, and C3 have the highest maximum G values, and samples KC3, G1, and A2 have the lowest maximum G values.

Plain CTMP reference samples, A1 and A2, had maximum G values of 72.6 G and 60.3 G, respectively. Reference A3 with the addition of 1% cationic starch, and reference A4 with the addition of 4% citric acid did not result in remarkable differences in the maximum G values compared to plain references, resulting in values of 62.7 G and 69.7 G, respectively. The results of other samples are compared to the average of two plain reference samples, 66.4 G. The results of plain reference samples shown in this subtitle, A1 and A2, were prepared two times, since the first obtained results had remarkably high differences in the results of resilience, and in order to obtain reliable results, the reference samples were prepared again. The results of strength and resilience for old and new A1 and A2 samples are shown in Table 2. The other obtained results are compared to the new references that show more comparable results. Together with CTMP references, the same tests were done for petroleum-based alternatives, EPS and PU, to see how well CTMP samples with additives perform compared to petroleum-based alternatives (Appendix F).

Table 2. Results of maximum G values and resilience after first and third drops for old and new CTMP reference samples A1 and A2.

Sample name	Maximum G value after 1 st drop	Maximum G value after 3 rd drop	Resilience after 1 st drop	Resilience after 3 rd drop
old A1	72.6	93.8	97.1%	95.3%
new A1	67.1	93.4	96.3%	93.8%
old A2	60.3	94.3	93.9%	90.4%
new A2	63.0	96.6	95.4%	92.7%

The highest maximum G values, over 100, after the first drop in drop tests were gained with the following samples: 20% HPH23 synthetic latex (SL2), 5% chitosan (C2), and 5% chitosan + 1% cationic starch (C3). Standard deviation of C2 shows that the data of the first drop of C2 samples is widely spread and is thus less reliable compared to results of SL2 and C3. The maximum G value of SL2 was 70% higher compared to the plain reference samples, and the maximum G values of C2 and C3 are 58% and 56% higher than the reference samples, respectively.

The lowest maximum G values of around 60 G after the first drop were obtained for sample with 4% citric acid (A4), 5% k-carrageenan (KC2), 0.5% k-carrageenan + 1% cationic starch (KC3), and 0.5% low molecular weight guar gum (G1). The maximum G value of KC2 is 8.5% lower compared to reference samples, and maximum G values of KC3 and G1 are 10.6% and 9.1% lower than references, respectively.

Samples HC1, HC2 and HC3 including differing amounts of HefCel together with the 1% addition of cationic starch show no remarkable difference between the maximum G values after the first drop. Samples KC1, KC2, KC3 and KC4 also did not have drastic changes between the maximum G values, but it is worth noticing that the density of KC4 is remarkably lower compared to other samples with k-carrageenan, about 61 kg/m³, whereas the density of other samples is from 71.5 to 73.2 kg/m³, and the maximum G value of KC4 is slightly higher compared to maximum G values of the other samples.

Eight different sampling points, including different types of guar gums, resulted in differing maximum G values. Samples G1 and G2 with low molecular weight guar gum had lower maximum G values, 60.4 G and 72.8 G, compared to samples G3 and G4 with high molecular weight guar gum with maximum G values of 77.3 and 83.2. However, G3 and G4 have higher densities compared to G1 and G2, which can also affect the results. It is also observed that samples with higher dosages of chemicals show higher maximum G values compared to samples with lower addition of chemicals. Samples including anionic guar gum, G5, G6, G7 and G8, had almost the same maximum G values after the first drop, values differing from 69 to 74. Samples G8 and G8 included cationic starch together with anionic guar gum to study whether the addition of cationic starch improves the results, but no remarkable difference could be seen.

The results after the third drop are presented in Figure 19. After three drops, the difference between the maximum G values in Z-direction is lower, and the change in maximum G values indicates that the structure of the samples changed because of mechanical stress acting on the material causing deformation. All maximum G values after the third drop were between 91.5 G and 113G, sample with the addition of 0.5% k-carrageenan (KC1) having the lowest, and the sample with the addition of 5% low molecular weight guar gum (G2) having the highest maximum G values.

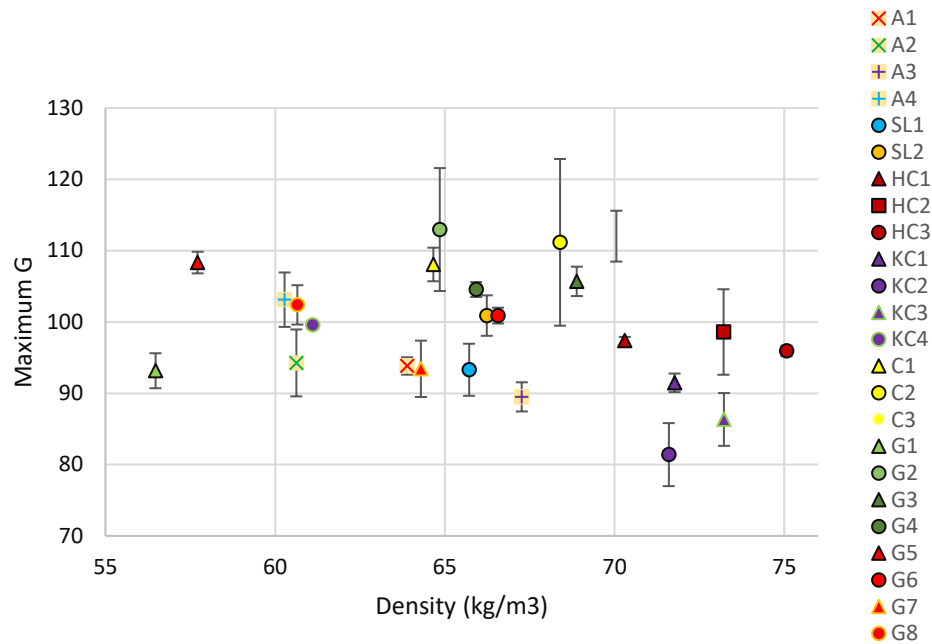


Figure 19. Maximum G values after the third drop in the Platen drop test. The maximum G values are closer to each other compared to results after the first drop.

Comparing the changes in the maximum G values between the first and third drops, it is noticed that samples with the highest G values after the first drop also displayed the lowest change in maximum G value (Figure 20). Reference samples A1 and A2 had a difference of 26.3 G and 33.6 G between the first and third drops, respectively.

Sampling point SL2 has differing results compared to other trial points, change being negative, -11.8 G, between first and third drop from 112.7 to 100.9 G. Samples C2, C3 and SL1 had the lowest difference between the first and third drops: 6.13 G, 8.59 G and 10.9 G, respectively. C1 with the lower dosage of chitosan expressed a difference of 19.5 G between the first and third drops, which is clearly higher compared to C2 and C3 with 10 times higher dosage of chitosan.

Slight difference could be noticed with the difference of maximum G values between the first and third drops of samples G1 and G2 compared to samples G3 and G4. Samples with high-molecular weight guar gum, G3 and G4, had lower difference between the

maximum G values of drops, 28.4 G and 21.4G, compared to G1 and G2, 32.8 G and 40.2 G.

It is observed that there were no remarkable differences between the maximum G values of first and third drops in other samples compared to the results of reference samples. The standard deviation of some of the results is relatively high, especially in the results of maximum G values after the first drop, but the standard deviation noticeably decreases in the results after the third drop, e.g., sample SL1 show a standard deviation of 12.1 G after the first drop, whereas the standard deviation after the third drop is 3.7 G.

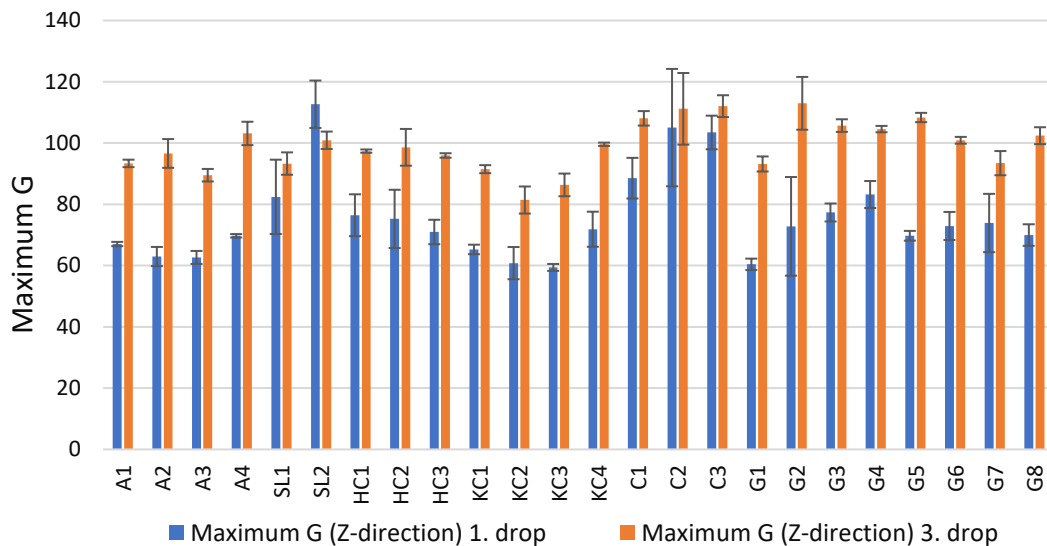


Figure 20. Maximum G values after the first and third drop together showing the change in the results between drops.

Results of resilience after the first drop are presented in Figure 21. The average resilience after the first drop for reference samples were: 95.9% (A1 and A2), 96.3% (A3), and 94.9% (A4).

The same samples that had a few of the highest maximum G values after the first drop, C2 and C3, showed the highest and fourth highest resilience of 97.8% (C2) and 96.9% (C3). In addition, samples KC4 and KC2 had second and third highest resilience after the

first drop, 96.9% and 97.1%. However, the density of KC2 is relatively high compared to other samples with the highest resilience, and in Figure 21 the focus is on the circled area that shows the samples with similar density, between 60 and 70 kg/m³ compared to the reference samples. Inside the circled area is also sample SL1, with a relatively high resilience of 96.6%, which is slightly higher than the resilience of plain references.

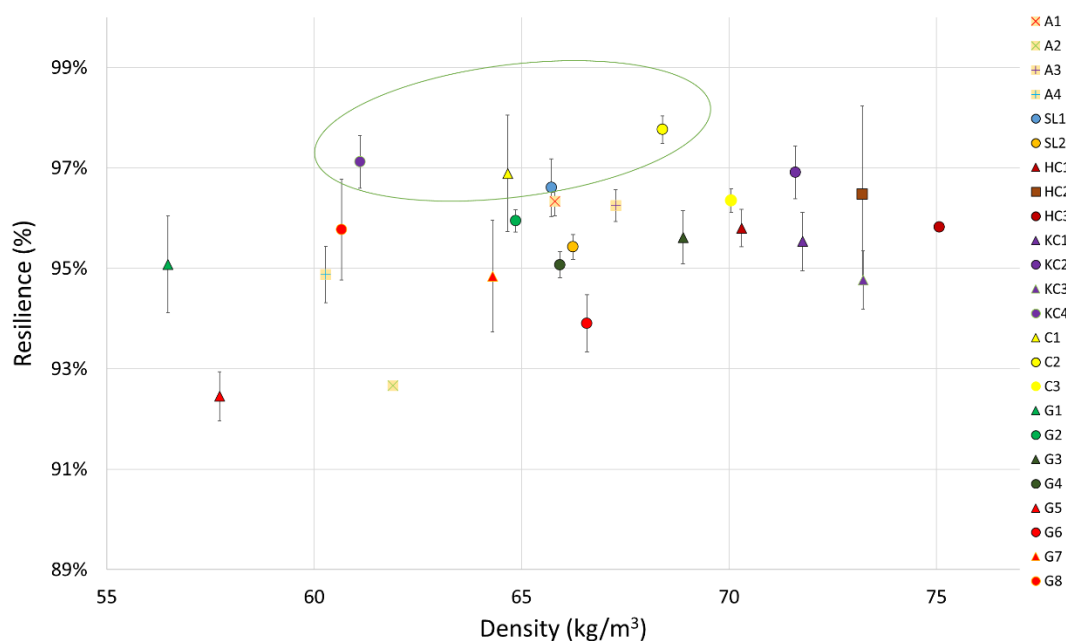


Figure 21. Results of resilience after the first drop. Circled area focusing on the samples with the highest resilience at a density between 60 and 70 kg/m³.

Sample G5 with lower addition of anionic guar gum shows the lowest resilience of 92.5% after the first drop, which is 3.6% lower compared to the resilience of reference samples, but it is worth emphasizing that the density of G5 is the second lowest, 57.7 kg/m³, which might affect the results. Surprisingly, the sample with the lowest density, G1, with a density of 56.5 kg/m³, resulted in notably high resilience of 95.1%. The resilience of G1 is 0.84% lower compared to the resilience of reference samples, but the density of G1 is also 11.6% lower compared to the references.

Results of resilience after three drops are presented in Figure 22. As in maximum G values, also in the results of resilience lower change between the results of first and third drop is better, since lower change indicates better resilience that does not decrease after many drops. The average resilience of reference samples A1 and A2 is 93%, thus the resilience has dropped 2.9% after the first drop. Resilience after three drops of A3 and A4 are 93.7% and 92.7%, so the results are 2.60% and 2.16% lower than after the first drop, respectively.

In Figure 22, the circled area shows the highest results of resilience above references for samples that have density between 60 kg/m^3 and 70 kg/m^3 . The highest resilience after three drops is observed for sample C2 with resilience of 96.2% after the third drop, and the difference after the first drop is -1.60%. C3 has second highest resilience of 92.96%. However, the difference in resilience between first and third drop for C3 is only -0.40%, which is the third lowest change in resilience. Also, the standard deviation of C3 is noticeably narrower compared to C2, thus the results are more reliable.

The third highest resilience after three drops was noticed with a sample that has a lower addition % of chitosan (0.5%), C1, resilience being 95.6%. Moreover, the samples that had the lowest resilience after three drops, were G5 (90.6%), KC3 (91.1%), and G1 (92.0%). The change of resilience between the first and third drop for these samples is -1.82%, -3.72%, and -3.08%, respectively.

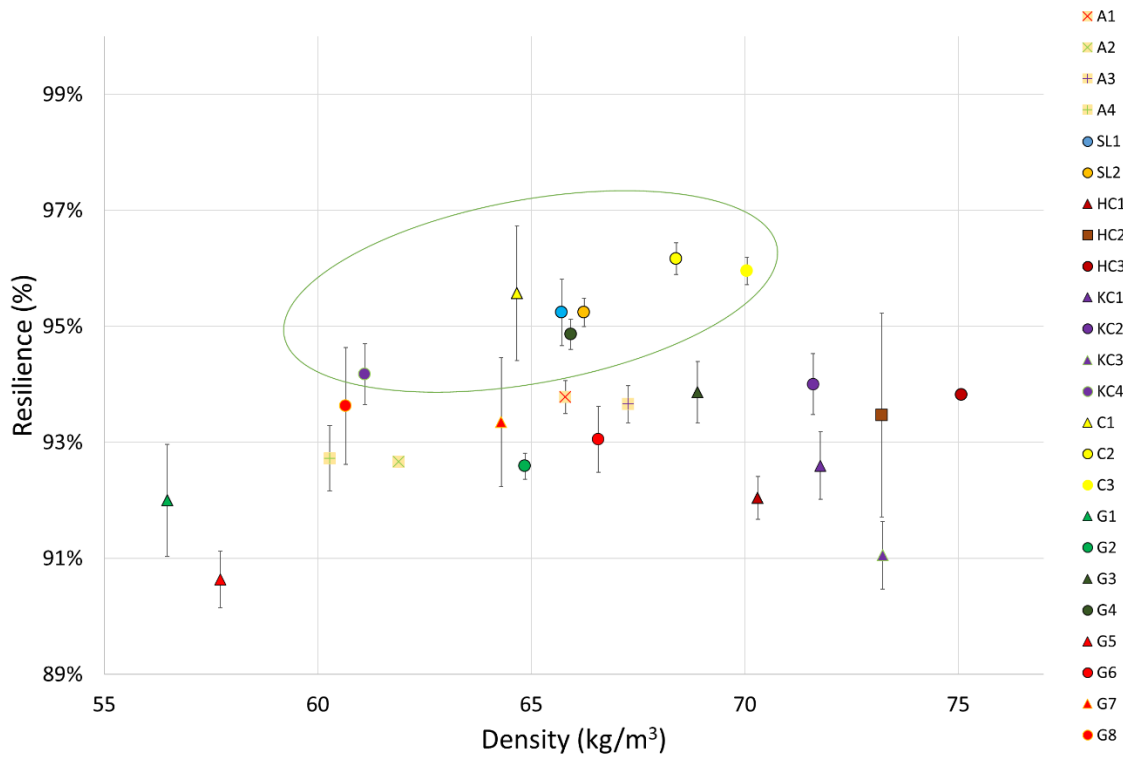


Figure 22. Resilience after the third drop. Circled area focusing on the samples that had the highest resilience after the third drop.

In Figure 23, the resilience of the samples is plotted against strain. The strain is defined by calculating maximum displacement divided by initial thickness, and resilience is calculated by dividing thickness after the drop by initial thickness. The figure represents a decreasing trend of higher resilience with lower strain and vice versa. R-squared value of the regression line is 0.57, which reveals that about 57% of the variability in the results of resilience could be explained by strain.

The samples with the lowest strain had the highest resilience (C2 and C3), and the samples with the highest strain showed lowest resilience (A2 and G5), thus moderate trend can be seen between lower strain and higher resilience.

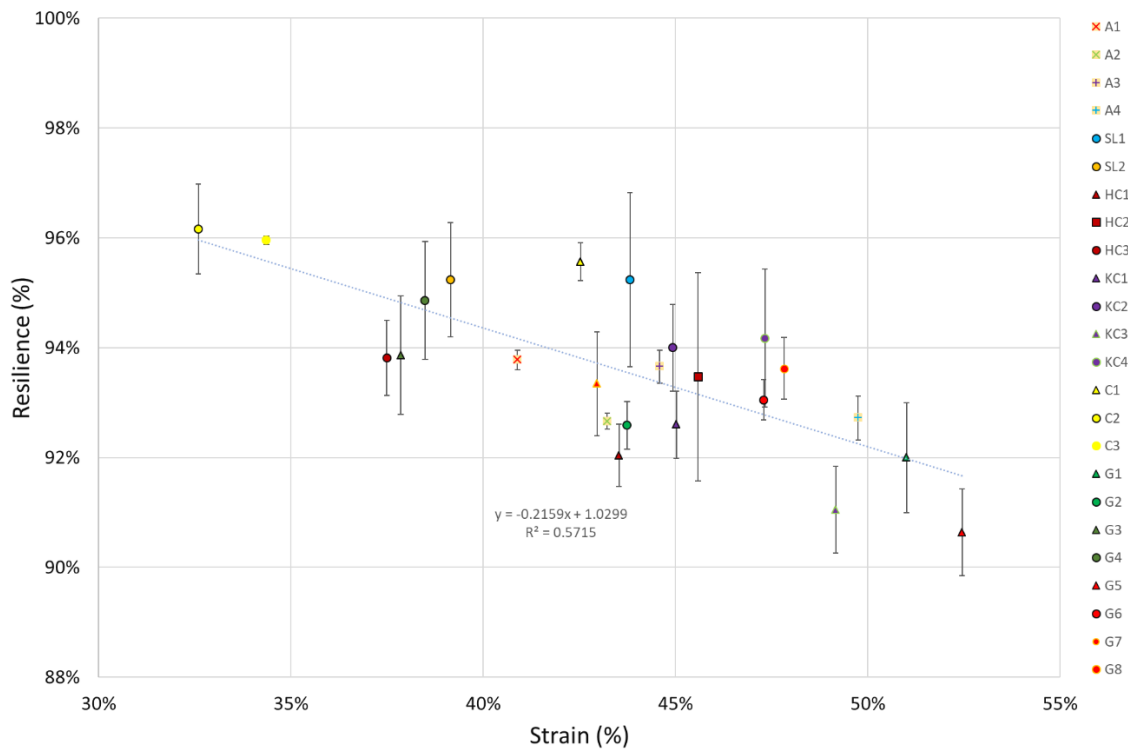


Figure 23. Resilience plotted against strain after the 3rd drop.

10.3 Drop test results – failure modes

Videos were obtained from the high-speed camera mainly to observe the maximum displacement from which strain (%) was calculated. In addition to maximum displacement, also fracture mechanisms of structures, and crack propagation directions could be roughly observed from the high-speed camera videos.

It was observed that the fracture of structures was the easiest to observe after the plate had hit the test specimen and bounced back up. The type of fracture varied between various samples, but the main fracture mechanism was observed to be opening mode, in which the applied stress is orthogonal to the local plane of the crack surface (Zehnder, 2013). The size or amount of failures, or cracks, increased the more drops had been done. The location and size of the cracks vary between samples with different types and amounts of additives (See Appendix H).

The samples that performed the best in drop tests, were decided to examine more closely together with a few reference samples. Plain references, A1 and A2, show clear opening

of cracks already after the first drop, and the size of the cracks increased after the third drop (Appendix H, Figure H1). Samples with synthetic latex, SL1 and SL2, display negligible failure, or failure that could not be observed from the high-speed camera videos (Appendix H, Figure H2 and H3). Sample KC4 shows no clear failures after the first drop, but many small cracks can be noticed on the bottom part of the sample after the third drop (Appendix H, Figure H4).

Samples C2 and C3 resulted in similar results in maximum G values and resilience with just slight differences, but it is noticed that sample C2 with the addition of 5% chitosan shows a long crack that “peels” off from the bottom already after the first drop, and the crack spreads even more after the third drop (Appendix H, Figure H5 and H6). Same type of fracture was observed with all three samples of C2 that were tested with Platen drop test. Sample C3 with the addition of 5% chitosan together with the addition of 4% citric acid displays no noticeable cracks or failures even after the third drop.

10.4 Results of micro-computed X-ray tomography

Samples that performed the best in drop tests, were chosen to be further analyzed with tomography and SEM imaging methods to see changes in the structures of the samples that could explain some of the results. Old and new plain reference samples, A1 and A2, were chosen to find an explanation for noticeable differences in the results of resilience. The selected samples were both synthetic latex samples, SL1 and SL2, together with samples including chitosan, which performed well in both, results of strength and resilience. These samples were chosen according to promising results. Additionally, one sample with addition of 5% k-carrageenan and 1% cationic starch, KC4, show relatively high resilience in lower density level was chosen together with other samples.

The list of samples that were analyzed with tomography are presented in Table 3. For every sampling point, except for plain reference samples, two 3D images were obtained from a tomographic scanner; one non-tested sample that displays the structure of the sample before mechanical testing, and one sample that has been through 3 drops in Platen drop test. The non-tested sample was different than the sample that was tested with Platen drop test.

Table 3. List of samples that were imaged with x-ray tomography.

	Additive	Addition of additive (%)	Addition of citric acid (%)	Addition of cationic starch (%)	Drop tests (amount)
Old A1	-	-	-	-	non-tested
New A1	-	-	-	-	non-tested
Old A2	-	-	-	-	non-tested
New A2	-	-	-	-	non-tested
Non-tested SL1	CHP557 Synthetic latex	20	-	-	non-tested
Tested SL1	HPH23 Synthetic latex	20	-	-	3 drops
Non-tested SL2	HPH23 Synthetic latex	20	-	-	non-tested
Tested SL2	HPH23 Synthetic latex	20	-	-	3 drops
Non-tested KC4	K-carrageenan	5	-	1	non-tested
Tested KC4	K-carrageenan	5	-	1	3 drops
Non-tested C1	Chitosan	0.5	-	-	non-tested
Tested C1	Chitosan	0.5	-	-	3 drops
Non-tested C2	Chitosan	5	-	-	non-tested
Tested C2	Chitosan	5	-	-	3 drops

Tomography images of plain reference samples (Figure 24) reveal variation in the pore size distribution, density distribution, and orientation of the fibres between the samples. In all reference samples, the top and bottom surfaces are denser compared to the middle

part of the samples, which is partly a result of gently pressing the foam with mesh and screen plate to get an even surface after pouring the foam into the sheet mold. It is noticed that the structure of old A1 is the most homogeneous out of all plain reference samples, which might explain some of the results of resilience. Old A2 had the poorest resilience of all plain reference samples and tomography image shows larger pores, and more heterogeneous structure. There is no remarkable difference between the internal structures of new A1 and A2 reference samples, and also the results of resilience and maximum G values were closer to each other.

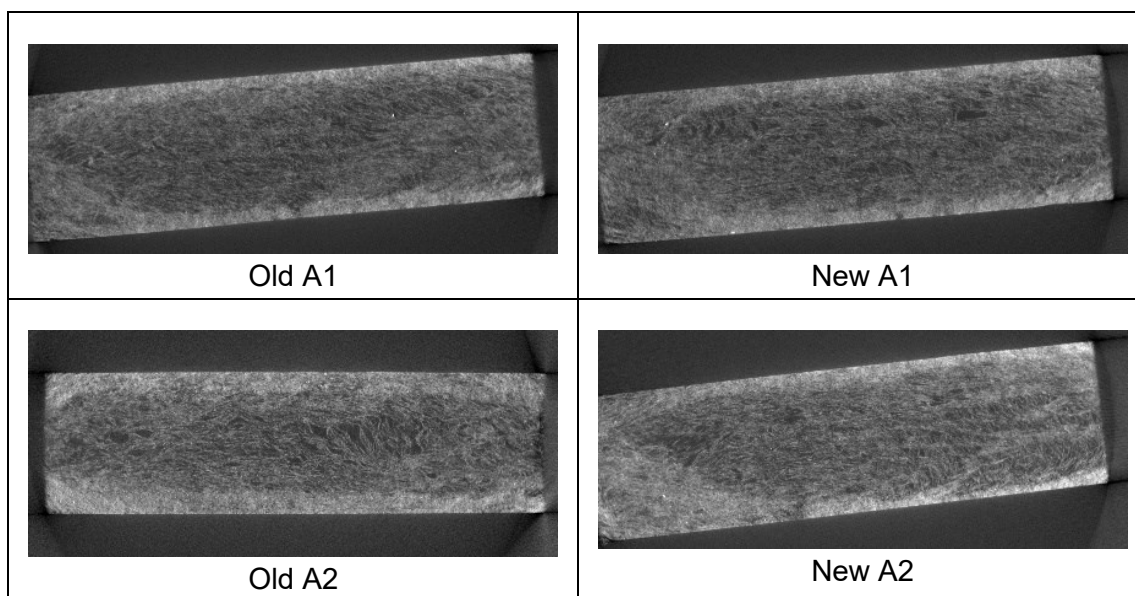


Figure 24. Tomography images showing internal structure of old and new plain reference samples, A1 and A2.

Samples including synthetic latex, SL1 and SL2, have no remarkable differences in their internal structures (Figure 25). Neither of the tested samples had noticeably compressed after three drops in mechanical testing compared to the non-tested samples.

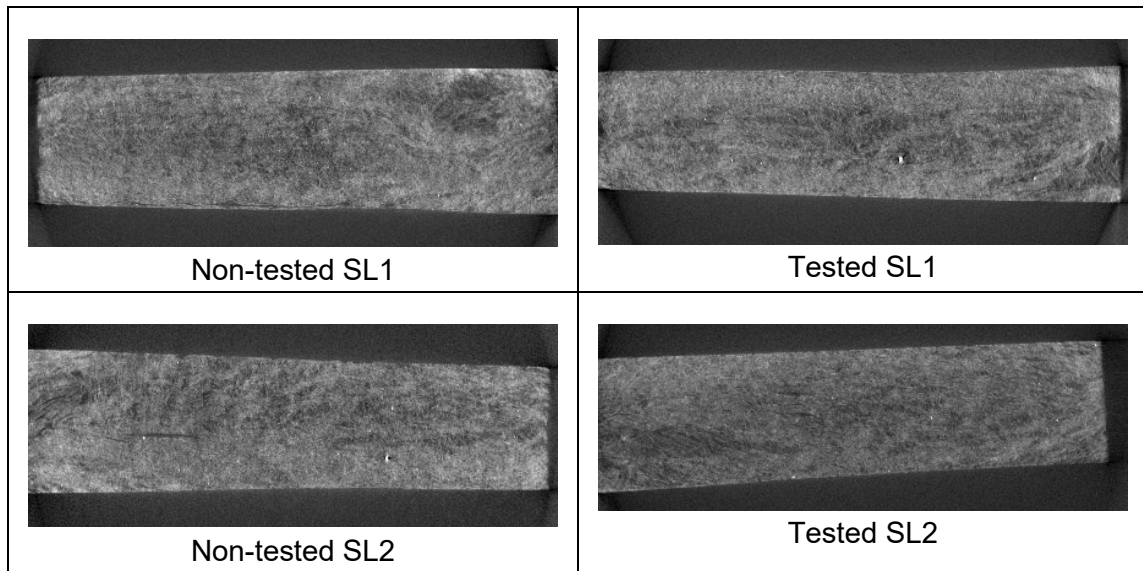


Figure 25. Tomography images show the internal structure of samples including synthetic latex, SL1 and SL2.

Tomography images of KC4 show remarkably different structures compared to other samples (Figure 26). The fibres have oriented in many different directions, the structure has large pores and wide pore size distribution, and also the density of the sample seems to vary noticeably. It is noticed that in the upper middle part of the non-tested sample, which is probably the point from which the foam has poured when the foam was generated, there are many vertically oriented fibres with large pores around. In the tomography image of the tested KC4 sample, this part is observably compressed, and the large pores have collapsed.

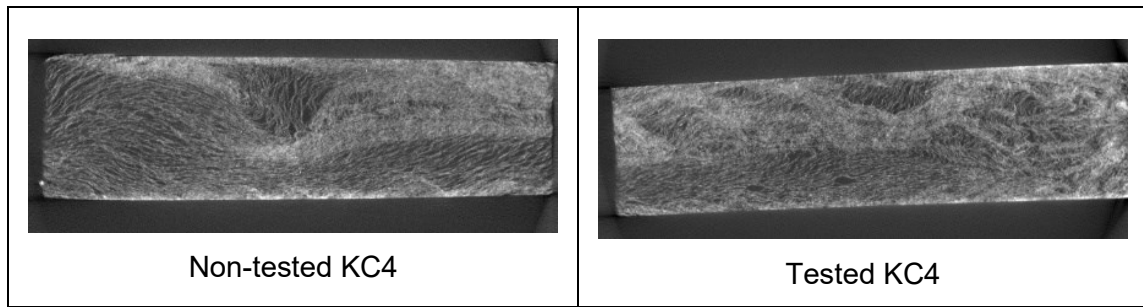


Figure 26. Tomography images of sample KC4 with addition of 5% k-carrageenan and 1% cationic starch show slight compression of the sample after three drops.

Sample with lower addition 0.5% of chitosan, C1, shows a more homogeneous structure in tomography images compared to the sample with higher addition 5% of chitosan, C2 (Figure 27). No remarkable difference is noticed between the tomography images of non-tested and tested C1 sample, and the internal structure of the sample looks the most homogeneous with even pore size distribution. The upper part of the internal structure of C2 looks homogeneous, but the lower part of the sample is not so dense compared to the upper part, and also the fibres have oriented more vertically throughout the bottom part of the sample. The non-tested C2 had a tiny failure, or crack, after preparation, that could be seen in the tomography images, thus it is slightly difficult to compare the differences between the non-tested and tested C2 samples, but no remarkable compression or other changes is noticed.

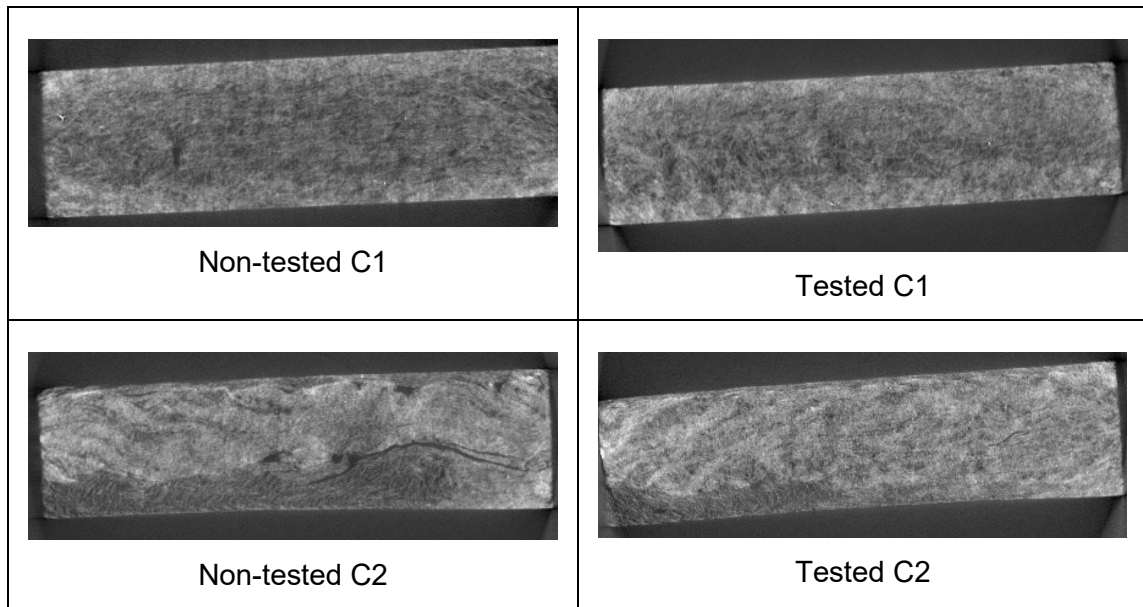


Figure 27. Tomography images of C1 with addition of 0.5% chitosan shows more homogeneous structure compared to C2 with 5% addition of chitosan.

10.4 Results of porosity profile and pore size distribution

From the obtained 3D tomography images, porosity profile and pore size distribution were calculated for some of the samples. Porosity profile (Figure 28) shows that the samples with the highest maximum G values and the highest resilience show more even porosity profiles. Also, as mentioned before, results of plain references A1 and A2 varied, and difference is noticed in the porosity profiles of the samples as well. The porosity profile of A2 shows a more porous middle part of the sample compared to the more even porosity of A1, which could explain the results of resilience. Samples that resulted in the highest results of maximum G values and resilience show lower porosity throughout the samples, samples including 5% of chitosan and samples with different types of synthetic latex.

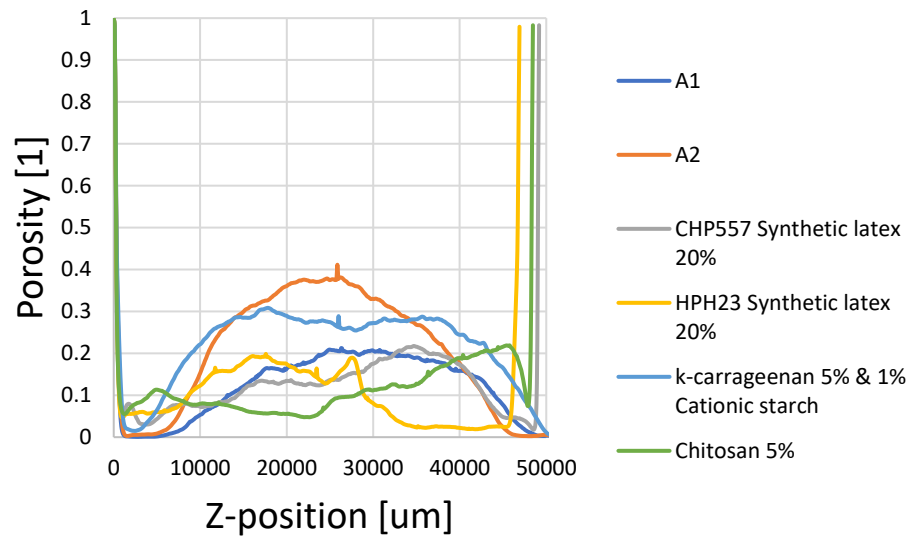


Figure 28. Porosity profile showing total porosity of the samples in the Z-direction from top to bottom part of the samples, from left to right.

Together with the porosity profile, also pore size distribution was calculated from the obtained 3D tomography images. Figure 29 presents the pore size distribution, and it is noticed, that the results vary between plain reference samples, A1 and A2. A1 includes more pores with smaller diameter compared to A2 with larger pores. Results show that out of samples with additives, the sample which included 5% of k-carrageenan together with 1% of cationic starch, KC4, have larger pores compared to samples with synthetic latex, SL1 and SL2, and chitosan, C2. This finding strengthens the assumption that a more homogeneous structure with more even pore size distribution results in better strength and resilience.

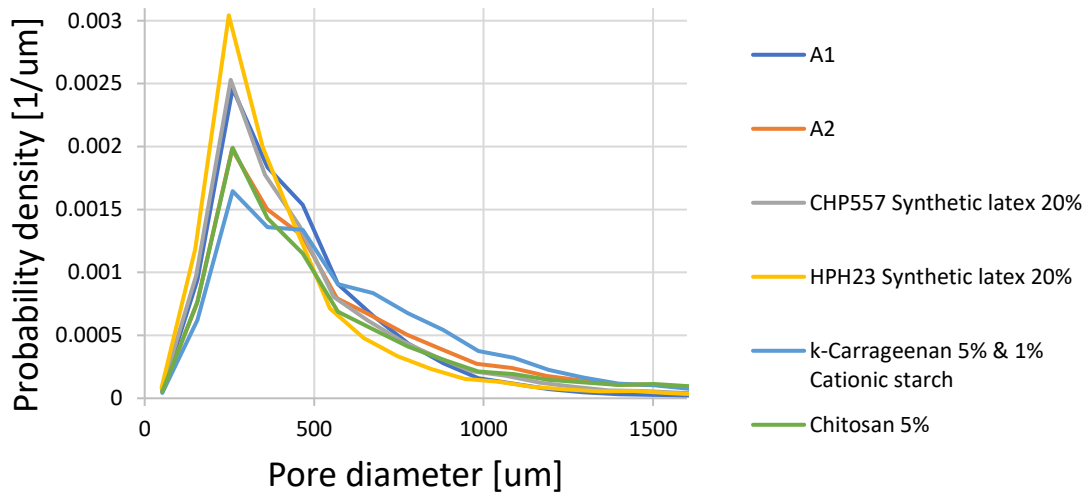


Figure 29. Pore size distribution of samples showing probability density as a function of pore diameter.

10.5 Results of SEM imaging

The same samples that were imaged with x-ray tomography, were imaged with SEM to obtain high-resolution images of the surfaces of the samples.

SEM images of reference samples, old A1, new A2, and new A2, are presented in Figure 30. Images show noticeable structural differences between the reference samples; newer A1 and A2 have more aggregated and bundled fibres compared to previously made A1 with more homogeneous structure and better separated fibres.

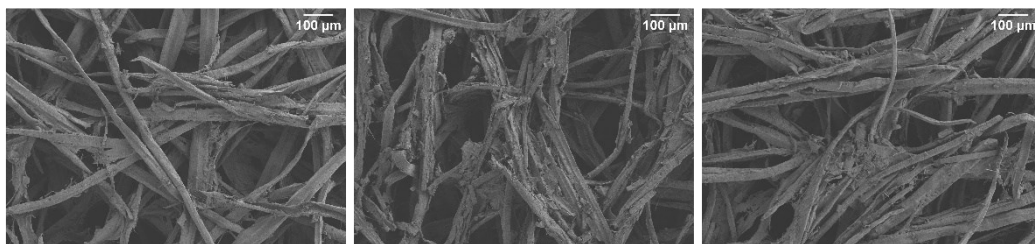


Figure 30. SEM images of old A1, new A1, and new A2 samples using the same magnification of 100x to show differences between the samples.

Samples SL1 (CHP557) and SL2 (HPH23) with synthetic latex did not reveal remarkable changes in the structure compared to reference samples with the magnification of 100x. However, with higher magnification of 1000x the surface of the fibres looks rougher, and tiny clusters, possibly synthetic latex particles, has gathered on some parts of the fibres (Figure 31Figure 32).

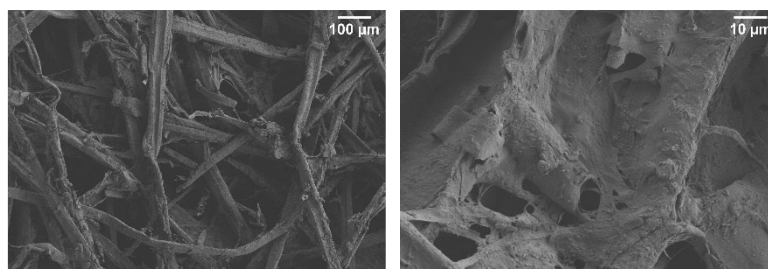


Figure 31. SEM images with magnification of 100x and 1000x showing the structure of SL1.

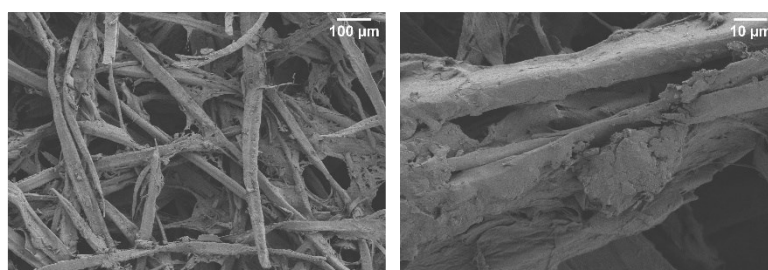


Figure 32. SEM images with magnification of 100x and 1000x showing the structure of SL2.

SEM-images of sample KC4 with 5% k-carrageenan and cationic starch (Figure 33) display that the chemical might not have distributed evenly throughout the sample, since clusters of assumably the used chemical, k-carrageenan, or cationic starch, could be seen on the surface of fibres.

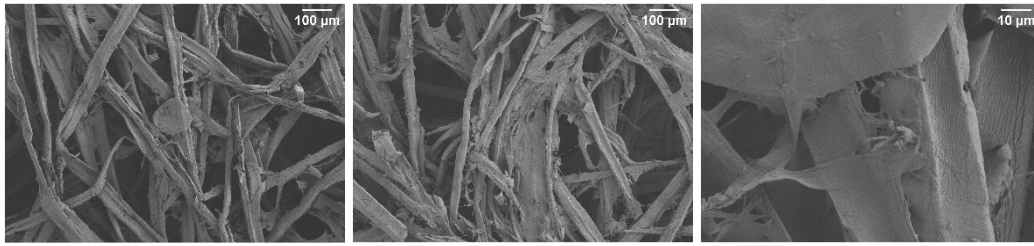


Figure 33. SEM images of KC4 (magnifications of 100x, 100x, 1000x) showing uneven distribution of k-carrageenan.

SEM images of the surface of samples C1 and C2 with chitosan (Figure 34) show a denser and rougher surface with a lot of fibres compared to reference samples. From tomography images, it was noticed that the density of these samples was not even, and the bottom of the sample was more porous compared to denser surface, so if SEM images were taken out of the bottom or middle part of the sample, the structure might look different.



Figure 34. Sample C1 (two first ones) and C2 (the last one) with magnification of 100x showing denser surface of the samples.

11 DISCUSSION

11.1 Effect of homogeneity and even distribution of fibres on the results

Two plain CTMP references, A1 and A2, were compared to the samples that included different additives. Due to the high variation in the reference samples (old A1 and old A2?), the reference samples were prepared again (new A1 and A2) to get more reliable and comparable results. It was observed that the new results of maximum G value and

resilience were more comparable with narrower standard distribution, increasing the reliability of the obtained results. Interestingly, one sample (old A1) had higher resilience than the other three reference samples. Therefore, the samples were analyzed more to explain the substantial difference in the results of resilience.

The possible explanation for the variation in resilience results could be found in the 3D tomography images. The structure of old A1 was more homogeneous, and the fibres were distributed more evenly throughout the sample, whereas old A2 had larger pores and wider pore size distribution, and the fibres had gathered in bundles around the pores and on the surface of the sample resulting in a structure that does not have even density throughout the sample. In addition, the new A1 and new A2 references also had relatively even and homogeneous structures, which probably led to closer results of maximum G values and resilience.

The reason for differences in the results could be partly in mechanical mixing when the foams were generated since even though four impellers were mixing the foam, air content was increased faster to the target level by manually moving the impellers up and down. In this case, foaming has not remained constant, and a higher amount of mechanical mixing might have led to some changes in the final structure, e.g., more separated, non-bundled and evenly distributed fibres. This could be further studied with foaming experiments to learn more about how to get repeatable, evenly distributed samples.

11.2 Results of strength and resilience compared to EPS and PU

When the target is to replace widely used petrochemical-based packaging cushioning materials, the main references usually are expanded polystyrene (EPS) and polyurethane (PU) foams, which have slightly different characteristics, even though both are used especially in small transportation packages (Seo et al., 2004).

It cannot be straight evaluated, if lower or higher maximum G value is better than another, since it depends on the packed item and the maximum G forces that it can stand. Commonly used EPS is stiff material, which results in higher maximum G values in the Platen drop test, whereas soft and elastic PU results in lower maximum G values. Tested EPS reference with average density of 20 kg/m³ has maximum Z-directional G-value of about 180 G that does not change drastically between the first and third drops, and tested

PU reference with average density of 28 kg/m^3 has maximum G values of about 40 G and 50 G after first and third drops, respectively (Appendix F, Table F1). Although EPS and PU have structural differences and differing G values, both materials recover almost perfectly after three drops in Platen drop tests, results of resilience being approximately 99% for PU and over 97% for EPS (Appendix F, Table F2).

Taking into consideration that the density of these reference materials (20 kg/m^3) is around three times smaller compared to the target density of the sheets prepared for the experiments in this study (60 kg/m^3), the resilience of reference materials is remarkably higher compared to the resilience of the prepared samples. EPS and PU materials are lightweight materials with excellent cushioning properties. EPS and PU materials are produced by polymerization reaction in which monomers are connected to one another forming a long polymer chain (Ghoreishi & Suppes, 2015; Hocking, 2005). Foam-formed materials also contain a connected network formed of fibres, but if the density is decreased without any other changes into the structure, the amount of bonds between the fibres is reduced as well, resulting in a weaker structure. Therefore, the addition of chemicals into the fibrous structure was studied to strengthen the structure and improve mechanical properties of foam-formed materials closer to EPS and PU.

11.3 The effect of different additives on strength and resilience

The highest maximum G values together with the highest resilience out of all trial points was gained with the addition of 5% chitosan (C3) and with addition of 5% chitosan and 4% citric acid (C4). The structure of these samples was stiffer, and more elastic compared to other samples. The mechanism behind the high stiffness and resilience of chitosan samples can be a result of the formation of hydrogen bonds between NH^{3+} ions from chitosan molecules and OH^+ from cellulose molecules. The amino groups of chitosan can be easily protonated, and form NH^{3+} in formic acid solution, and since chitosan solution was prepared in acetic acid, the formation of a hydrogen bond between hydroxyl groups of cellulose and amino groups of chitosan is possible. Also, electrostatic interaction is another possible mechanism that may affect the strength of the structure. (Zhang et al., 2020)

Wu et al. (2022) used chitosan (10-50%) together with polyacrylamide-cPAM (0.3-2.0%) to improve mechanical strength of foam-formed structures made of bleached softwood Kraft pulp (BSKP) and sodium dodecyl sulphate (SDS) as foaming agent. The results show high mechanical strength for samples with density below 60 kg/m³. The compressive stress of the sample with a 50% addition of chitosan was over 6 times higher compared to the reference sample, and with low addition of cPAM (0.5%). The sample with lower addition of chitosan (20%) showed almost the same improvement in compression stress. In this thesis, a relatively low amount of chitosan (0.5% and 5%) was used, but according to the results from Wu et al. (2022), a higher addition of chitosan together with cPAM or other cationic polymers could result in higher mechanical strength of foam-formed structures. The influence of pH was not studied in this thesis, but Myllytie et al., 2009 have studied the influence of pH on the interaction of chitosan with cellulose. They found that viscoelastic properties together with swelling of the adsorbed chitosan layer on cellulose were strongly influenced by pH, and with pH adjustment, the strengthening effect could be adjusted even more.

From tomography images it was observed that the internal structure of samples including chitosan was more homogeneous compared to CTMP reference samples, and results of pore size distribution revealed more evenly divided pores throughout the sample including chitosan. This finding might explain the better results of strength and resilience, and more evenly distributed pores led to more evenly distributed non-bundled fibres, which increased the interfibre contact area. Even though only minor differences were noticed between the resilience of C2 and C3, the high-speed camera revealed that C3 including citric acid as a crosslinker together with chitosan showed no noticeable failures after drops. Sample C2 without citric acid displayed a long crack along the bottom part of the sample. Consequently, using citric acid as a crosslinker together with chitosan might lead to stronger material, which could be further studied with a higher number of drops. Overall, samples including chitosan led to best results of strength and resilience.

In this thesis, the addition of synthetic latex led to good strength and resilience properties. Paunonen et al., 2018 suggested that using elastic, polymeric components together with cellulosic fibres in foam forming could help the fibrous network to recover after deformation. Based on their study, the polymeric components would gather in the fibre joints during the drying of fibrous structures. They found that the distribution of natural

rubber latex was accumulated at fibre joints. Finding from their study could be one possible mechanism for improvement of strength when using synthetic latex in foam-formed structures. SL1 and SL2 with 20% addition of synthetic latex resulted in high maximum G values indicating that the structure was more rigid and better comparable with EPS.

From the drop test results, sample SL2 with 20% addition of synthetic latex (HPH23), was the only sample in which the maximum G value decreased between 1st and 3rd drops. The explanation for this could be that the structure of SL2 might have changed more drastically during the first drop compared to the other tested samples; if synthetic latex formed bridges in the structure, these bridges might have broken after the first drop. SL1 with 20% addition of CHP557 synthetic latex resulted in moderately lower maximum G values compared to SL2. The high-speed videos after drop tests revealed no noticeable failures in the structures, and tomography images together with results of pore size distribution displayed more homogeneous structures with relatively even pore size distribution compared to reference samples. As Paunonen et al., 2018 estimated, gathering of polymer components into fibre joints could lead to better recovery of fibrous structures, and even though this finding could not be verified well from the SEM images, accumulation of synthetic latex at fibre joints is one feasible mechanism to explain improved strength and resilience.

Cellulose nanofibrils (CNF) have been proven to increase the strength properties of foam-formed fibrous structures, and Torvinen & Lahtinen (2015) found that the addition of 2-6% CNF can improve the z-strength of foam-formed materials with 14-50% while still maintaining excellent formation. The results from drop tests reveal that samples including HefCel (HC1, HC2 and HC3) resulted in almost the same maximum G values and resilience compared to reference samples (A1 and A2), and no clear improvement of mechanical properties was found. In all of these trial points (HC1, HC2 and HC3) the same amount of cationic starch was used even though the amount of HefCel was changed, which could have led to lower retention of anionic CNF on the fibre surface. The poor retention or the lack of bonding with wood fibres could explain the results of strength and resilience that were not changed excessively between samples including HefCel.

One of the selected additives in this study was k-carrageenan. From the drop test results, samples with k-carrageenan (KC1, KC2, KC3 and KC4) displayed the lowest maximum G values compared to the average maximum G values of different samples. The results indicate softer material. However, one sample, KC4: 5% k-carrageenan + 1% cationic starch, maintained relatively good resilience (94.2% in density of 61 kg/m³) after the third drop. In this trial point, the addition of cationic starch probably improved the strengthening effect of k-carrageenan. This can be concluded from the results of KC4 with cationic starch, which was compared to KC2 with the same amount of k-carrageenan without cationic starch; the resilience was on the same level even though the density of KC4 was lower (61 kg/m³) compared to KC2 (72 kg/m³). Tomography images revealed divergent structure for KC4 with larger pores and varying orientation of the fibres, and results of porosity profile also showed rather high porosity throughout the sample with larger pores in pore size distribution. The high viscosity of the used k-carrageenan solution might explain some of the results, and SEM images revealed “clumps” of some chemical on the surface of the fibres indicating possibly uneven distribution of either k-carrageenan or cationic starch.

Liu et al. (2017) have studied the use of carrageenan as a dry strength additive in papermaking, and they prepared hand sheets with a target grammage of 70 g/m². They obtained that with optimal carrageenan dosage of 0.2%, the tensile index was 25.68% higher compared to samples without carrageenan. They obtained SEM images that displayed smoother and denser surface in samples with carrageenan compared to samples without carrageenan. More homogeneous structure usually indicates higher mechanical strength for fibrous structures, and according to the results, carrageenan as a dry strength additive could improve mechanical strength also with foam-formed structures. Even though in the study of Liu et al. (2017) carrageenan improved the tensile strength of paper, it was expected that k-carrageenan could have strengthening effect on the foam-formed structures as well. Moderate improvement of strength properties was observed with foam-formed samples including k-carrageenan, but more evenly distributed structure could have led to better results of strength and resilience as observed with samples including chitosan and synthetic latex.

Eight samples with three different types of guar gum with and without of cationic starch resulted in only slightly differing results. Guar gum has been well-established as a

retention aid in traditional papermaking before, as it can improve drainage and retention together with increasing the mechanical strength of the structure (Lindqvist et al., 2013). Samples with high molecular weight guar gum (G3 and G4) showed higher resilience compared to low molecular weight guar gum samples (G1 and G2). Also, the change between the maximum G values of first and third drops in drop tests was lower for G3 and G4 compared to G1 and G2 indicating that the structure of samples with high molecular weight guar gum withstands shocks slightly better. However, the density of G1 and G2 was slightly lower compared to G3 and G4, and if the results were compared at the same density level, the difference between high and low molecular weight guar could be smaller.

Samples including anionic guar gum without crosslinker, cationic starch (G5 and G6), did not result in remarkably different results of strength and resilience compared to samples with anionic guar gum and cationic starch (G7 and G8). A comparison of higher addition level, 5%, of anionic guar gum without and with crosslinker shows that the difference is so minor that the addition of cationic starch did not seem to have clear effect. However, comparing the samples with lower addition level, 0.5%, of anionic guar gum without crosslinker (G5) and with crosslinker (G7), the change in the results is observed. The difference between the maximum G value of the first and third drop was lower for G7, which means that structure of G7 withstands mechanical stress better compared to G5. Also, the recovery of G5 is lower (90.6%), compared to G7 (93.3%) after the third drop. No further characterization was done for samples including guar gum since the results were not remarkably different compared to the reference. It can be concluded, that using cationic starch as a crosslinker with guar gum can improve the strength and resilience.

11.4 Potential replacement of cushioning materials

The results from the Platen drop test show that the strength and recovery of fibre-based materials with different additives are not yet on the same level compared to EPS or PU materials. However, regulations are constantly getting stricter and focusing on more sustainable solutions. Therefore, if fossil fuel -based cushioning materials must be reduced at some point, alternative environmentally friendly solutions are needed. In this case, theoretically, slightly lower results of strength and resilience could be compensated by packaging design and keeping environmental impact as minimal as possible.

The highest resilience after the first drop was achieved with sample C2 including 5% of chitosan with resilience of 96.2% at a density level of 68 kg/m³. However, when this result is compared with commonly used cushioning materials EPS and PU, with resilience of approximately 97-99% with density level of 20 kg/m³, more improvement is still needed to get mechanical properties of foam-formed materials closer to EPS and PU. On the other hand, when comparing the results of sample C2 to the plain CTMP references A1 and A2, the resilience after the third drop was improved 2.95%, thus clear improvement can be noticed compared to reference samples without additives. Nevertheless, there is still a question if the level of resilience is enough for packaging cushioning applications. Conclusions cannot be drawn clearly from the results of maximum G values since the desired maximum G value depends on the packed item that must be protected.

In this thesis, the bio-based content or recyclability of the used chemicals was not the limiting factor, although recyclability and ecology of the selected chemicals were considered. E.g., Ottenhall et al., 2018 have studied the stability of cellulose fiber foams in water, and they found that foam containing chitosan and citric acid did not disintegrate in water even after vigorous shaking for 18 hours, thus resulting in relatively water-resistant foam. According to this study, even though the foam-formed samples including chitosan highly improved the strength and resilience of fibre-based foam-formed structures, the amount of chitosan must be optimized to get a material that is mechanically strong, but also possible to be recycled.

11.5 Challenges and uncertainties

In view of the fact that experimental work included an extensive set of data with varying variables, the causality of the results can be hard to estimate. Difficulty in preparation of the samples varied between the samples, and e.g., generating homogeneous foam including k-carrageenan was more challenging due to the high viscosity. In addition, some “clumps” seen in SEM images may indicate improper distribution of additives throughout the sample. Also, foaming time varied between the samples, and this might have affected the drainage and pore size distribution of the samples. Samples that included citric acid, reference A4 and C17 with addition of 5% chitosan, were heat-treated to crosslink the structure. To reveal if crosslinking has happened, further studies with FT-IR spectroscopy could be recommended. In the study, the results were not highly different

when comparing the results of C16 without citric acid and C17 with citric acid, and the reason for this could be improper crosslinking.

The CTMP reference samples were the only samples that were prepared twice, and high variation was observed in the structures of CTMP references, thus further studying is needed to prepare repeatable, even structures. The Platen drop test conditions were relatively harsh (drop height of 84.5 cm and dropped plate with a mass of 3.53 kg), which also increases the difference of results compared to EPS and PU.

Some parameters in drop tests were measured manually, thus this might have led to instrumental errors. The maximum displacement was roughly measured from videos obtained from the high-speed camera, and the thickness of the samples was measured with a caliper from four different corners of each sample. Precise measurement of drop height was slightly challenging, thus there might have been a few millimeters error in the drop height between different samples, which should not have affected the results remarkably.

12 CONCLUSION

This thesis demonstrated feasible strengthening additives, and their effects on the strength and resilience of foam-formed cushioning materials that were prepared from CTMP fibres. The results from the Platen drop test show that many chemicals improved the strength properties of the final structure, and the structures with chitosan (0.5%, 5%) and synthetic latex (20%) resulted in the most promising results in general. Slight improvement of strength and resilience was observed with some other samples, e.g., sample with k-carrageenan (5%) + cationic starch (1%). Recalling the aim of this thesis, how strength and resilience can be maximized, what are the main factors to affect these characteristics, and how different additives affect these characteristics, it can be concluded that the work partly answered the research questions. As main outcome, it was found that more homogeneous and rigid structures with more even pore size distribution led to the best results of strength and resilience. However, more specific research is still needed to confirm the hypothesis, since the used characterization

methods could not clearly verify the formation of new bonds, accumulation of polymers into the fibre joints, or retention of additives.

One of the next steps in research could be to study the recyclability of the produced samples, and to study if e.g., the amount of synthetic latex could be reduced or changed to bio-based alternative, like natural rubber latex. The number of drop tests performed in this work was rather limited, hence more drop tests could be performed to see if the results change drastically.

Also, the effect of foaming time could be compelling to study, if changing the foaming time affects e.g., pore size distribution and size of the pores. In the trials, the initial target density was 60 kg/m^3 , but the amounts of used chemicals were decided to add in addition to the same amount of fibres, which resulted in differing densities. It could be further studied, if normalizing the density is possible, and if this affected the results of maximum G values and resilience.

In addition to tomography and SEM imaging, FT-IR spectroscopy could also be one characterization tool to further study the formation of new bonds. Zeta potential measurements could also be one tool to study the change of charge density and the effects of additives on the fibres.

Even though the causality of some of the results could not be confirmed, this thesis accomplished its aim to understand better what affects the strength properties of foam-formed structures and generated more knowledge about different additives and their effects on the strength properties of foam-formed structures. The extensive set of experiments together with the collected data open up a new pathway for further research and drive upcoming research to better optimization of the structures. As an outcome of this work, we are one step closer to accomplish similar mechanical properties as fossil-fuel based cushioning, and one step closer to having more environmentally friendly packaging alternatives.

REFERENCES

- Adams, F., & Barbante, C. (2015). Chapter 2 - Spatially Confined Analysis. In F. Adams & C. Barbante (Eds.), *Chemical Imaging Analysis* (Vol. 69, pp. 29–66). Elsevier. <https://doi.org/https://doi.org/10.1016/B978-0-444-63439-9.00002-5>
- Alava, M., & Niskanen, K. (2006). The physics of paper. *Reports on Progress in Physics*, 69(3), 669.
- Amann, M., & Minge, O. (2011). Biodegradability of Poly(vinyl acetate) and Related Polymers (pp. 137–172). https://doi.org/10.1007/12_2011_153
- Andrieux, S. (2019). Theoretical Background (pp. 9–48). https://doi.org/10.1007/978-3-030-27832-8_2
- ASTM International. (2021). ASTM D1596-14 Standard Test Method for Dynamic Shock Cushioning Characteristics of Packaging Material. <https://doi.org/10.1520/D1596-14R21>
- Atri, M. R., & Ashrafizadeh, S. N. (2010). THE IMPORTANCE OF FOAMS AND ANTIFOAMING IN BIOPROCESSES. *J. Biotechnol*, 7(2), 19–39.
- Beil, N. B., & Roberts Jr, W. W. (2002). Modeling and Computer Simulation of the Compressional Behavior of Fiber Assemblies: Part I: Comparison to van Wyk's Theory. *Textile Research Journal*, 72(4), 341–351.
- Burgess, G. (1988). Product fragility and damage boundary theory. *Packaging Technology and Science*, 1, 5–10.
- Burgess, G. (1994). Generation of cushion curves from one shock pulse. *Packaging Technology and Science*, 7(4), 169–173. <https://doi.org/10.1002/pts.2770070403>
- Burke, S. R., Möbius, M. E., Hjelt, T., & Hutzler, S. (2019). Properties of lightweight fibrous structures made by a novel foam forming technique. *Cellulose*, 26(4), 2529–2539. <https://doi.org/10.1007/s10570-018-2205-5>
- Burke, S. R., Möbius, M. E., Hjelt, T., Ketoja, J. A., & Hutzler, S. (2021). Analysis of the foam-forming of non-woven lightweight fibrous materials using X-ray tomography. *SN Applied Sciences*, 3(2), 192. <https://doi.org/10.1007/s42452-021-04172-9>
- Callen, H. B. (1991). *Thermodynamics and an Introduction to Thermostatistics* (2nd ed.). John Wiley & Sons.
- Dennis, W. T. (2011). *Parcel and Small Package Delivery Industry*.
- Department of Defence. (1997). *Department of defense handbook - Package cushioning design, MIL-HDBK-304B*.

- di Maio, E., Iannace, S., & Mensitieri, G. (2021). Chapter 1 - Foams and their applications. In E. di Maio, S. Iannace, & G. Mensitieri (Eds.), *Foaming with Supercritical Fluids* (Vol. 9, pp. 1–20). Elsevier.
<https://doi.org/https://doi.org/10.1016/B978-0-444-63724-6.00001-9>
- Exerowa, D., & Kruglyakov, P. M. (1998). Chapter 1 - Formation and Structure of Foams. Pressure in the Liquid and Gas Phases of Foams. In D. Exerowa & P. M. Kruglyakov (Eds.), *Foam and Foam Films* (Vol. 5, pp. 1–41). Elsevier.
[https://doi.org/https://doi.org/10.1016/S1383-7303\(98\)80004-5](https://doi.org/https://doi.org/10.1016/S1383-7303(98)80004-5)
- Ferreira, F. v, Otoni, C. G., de France, K. J., Barud, H. S., Lona, L. M. F., Cranston, E. D., & Rojas, O. J. (2020). Porous nanocellulose gels and foams: Breakthrough status in the development of scaffolds for tissue engineering. *Materials Today*, 37, 126–141. <https://doi.org/https://doi.org/10.1016/j.mattod.2020.03.003>
- Flink, P., Westerlind, B., Rigdahl, M., & Stenberg, B. (1988). Bonding of untreated cellulose fibers to natural rubber. *Journal of Applied Polymer Science*, 35(8), 2155–2164. <https://doi.org/10.1002/app.1988.070350815>
- Fornué, E. D., Allan, G. G., Quiñones, H. J. C., González, G. T., & Saucedo, J. T. (2011). Fundamental aspects of adhesion between cellulosic surfaces in contact - A review. *O Papel*, 72, 85–90.
- Ghoreishi, R., & Suppes, G. J. (2015). Chain growth polymerization mechanism in polyurethane-forming reactions. *RSC Advances*, 5(84), 68361–68368.
<https://doi.org/10.1039/C5RA10725C>
- Goodwin, D., & Young, D. (2010). *Protective Packaging for Distribution: Design and Development*. DEStech Publications, Inc.
- Hamzeh, Y., Sabaghi, S., Ashori, A., Abdulkhani, A., & Soltani, F. (2013). Improving wet and dry strength properties of recycled old corrugated carton (OCC) pulp using various polymers. *Carbohydrate Polymers*, 94, 577–583.
<https://doi.org/10.1016/j.carbpol.2013.01.078>
- Hjelt, T., Ketoja, J. A., Kiiskinen, H., Koponen, A. I., & Pääkkönen, E. (2021). Foam forming of fiber products: a review. *Journal of Dispersion Science and Technology*, 1–37. <https://doi.org/10.1080/01932691.2020.1869035>
- Hocking, M. B. (2005). Commercial Addition (Vinyl-Type) Polymers. In *Handbook of Chemical Technology and Pollution Control* (pp. 737–758). Elsevier.
<https://doi.org/10.1016/B978-012088796-5/50026-0>
- Hou, Q., & Wang, X. (2017). The effect of PVA foaming characteristics on foam forming. *Cellulose*, 24(11), 4939–4948. <https://doi.org/10.1007/s10570-017-1452-1>
- Hubbe, M., Nanko, H., & McNeal, M. (2009). Retention aid polymer interactions with cellulosic surfaces and suspensions: A review. *BioResources*, 4(2), 850–906.
<https://doi.org/10.15376/biores.4.2.850-906>

- Ketoja, J., Paunonen, S., Jetsu, P., & Pääkkönen, E. (2019). Compression Strength Mechanisms of Low-Density Fibrous Materials. *Materials*, 12(3), 384. <https://doi.org/10.3390/ma12030384>
- Kidner, T. L. W. (1974, December). The radfoam process for fine papers. *Paper Technology*, 346–351.
- Kinnunen, K., Lehmonen, J., Beletski, N., Jetsu, P., & Hjelt, T. (2013). Benefits of foam forming technology and its application in high MFC addition structures. *Advances in Pulp and Paper Research*, 837–850.
- Kjellgren, H., Gällstedt, M., Engström, G., & Järnström, L. (2006). Barrier and surface properties of chitosan-coated greaseproof paper. *Carbohydrate Polymers*, 65(4), 453–460. <https://doi.org/https://doi.org/10.1016/j.carbpol.2006.02.005>
- Komori, T., & Makishima, K. (1977). Numbers of Fiber-to-Fiber Contacts in General Fiber Assemblies. *Textile Research Journal*, 47(1), 13–17. <https://doi.org/10.1177/004051757704700104>
- Kumagai, A., Tajima, N., Iwamoto, S., Morimoto, T., Nagatani, A., Okazaki, T., & Endo, T. (2019). Properties of natural rubber reinforced with cellulose nanofibers based on fiber diameter distribution as estimated by differential centrifugal sedimentation. *International Journal of Biological Macromolecules*, 121, 989–995. <https://doi.org/10.1016/j.ijbiomac.2018.10.090>
- Laleg, M., & Pikulik, I. I. (1991). Wet-web strength increase by chitosan. *Nordic Pulp & Paper Research Journal*, 6(3), 99–103. <https://doi.org/doi:10.3183/npprj-1991-06-03-p099-103>
- Laleg, M., & Pikulik, Z. I. (1993). Unconventional strength additives. *Nordic Pulp & Paper Research Journal*, 8(1), 41–47. <https://doi.org/doi:10.3183/npprj-1993-08-01-p041-047>
- Landis, E. N., & Keane, D. T. (2010). X-ray microtomography. *Materials Characterization*, 61(12), 1305–1316. <https://doi.org/https://doi.org/10.1016/j.matchar.2010.09.012>
- Landrock, A. H. (1995). *Handbook of plastic foams: types, properties, manufacture and applications*. Elsevier.
- Lappalainen, T., Salminen, K., Kinnunen, K., Järvinen, M., Mira, I., & Andersson, M. (2014a). Foam forming revisited. Part II. Effect of surfactant on the properties of foam-formed paper products. *Nordic Pulp & Paper Research Journal*, 29(4), 689–699. <https://doi.org/doi:10.3183/npprj-2014-29-04-p689-699>
- Lappalainen, T., Salminen, K., Kinnunen, K., Järvinen, M., Mira, I., & Andersson, M. (2014b). Foam forming revisited: Part II. Effect of surfactant on the properties of foam-formed paper products. *Nordic Pulp and Paper Research Journal*, 29(4), 689–699. <https://doi.org/10.3183/NPPRJ-2014-29-04-p689-699>

- Lecourt, M., Pöhler, T., Hornatowska, J., Salmén, L., & Jetsu, P. (2018). Density profiles of novel kraft pulp and TMP based foam formed thermal insulation materials observed by X-ray tomography and densitometry. *Holzforschung*, 72(5), 397–403. <https://doi.org/doi:10.1515/hf-2017-0116>
- Lehmonen, J., Retulainen, E., Kraft, M., Paltakari, J., & Kinnunen-Raudaskoski, K. (2020). Foam Forming under Dynamic Conditions. *BioResources*, 15(3), 6309–6331.
- Lehmonen, J., Retulainen, E., Paltakari, J., Kinnunen-Raudaskoski, K., & Koponen, A. (2020). Dewatering of foam-laid and water-laid structures and the formed web properties. *Cellulose*, 27(3), 1127–1146. <https://doi.org/10.1007/s10570-019-02842-x>
- Li, A., Xu, D., Luo, L., Zhou, Y., Yan, W., Leng, X., Dai, D., Zhou, Y., Ahmad, H., Rao, J., & Fan, M. (2021). Overview of nanocellulose as additives in paper processing and paper products. *Nanotechnology Reviews*, 10(1), 264–281. <https://doi.org/doi:10.1515/ntrev-2021-0023>
- Li, H., Du, Y., & Xu, Y. (2004). Adsorption and complexation of chitosan wet-end additives in papermaking systems. *Journal of Applied Polymer Science*, 91(4), 2642–2648. <https://doi.org/10.1002/app.13444>
- Li, H., Du, Y., Xu, Y., Zhan, H., & Kennedy, J. F. (2004). Interactions of cationized chitosan with components in a chemical pulp suspension. *Carbohydrate Polymers*, 58(2), 205–214. <https://doi.org/https://doi.org/10.1016/j.carbpol.2004.06.044>
- Liu, Z., Li, X., & Xie, W. (2017). Carrageenan as a dry strength additive for papermaking. *PLOS ONE*, 12(2), e0171326. <https://doi.org/10.1371/journal.pone.0171326>
- Malton, S., Kuys, K., Parker, I. H., & Vanderhoek, N. (1998). Adsorption of cationic starch on eucalypt pulp fibres and fines. *Appita Journal*, 292 – 298.
- McMullan, D. (2006). Scanning electron microscopy 1928-1965. *Scanning*, 17(3), 175–185. <https://doi.org/10.1002/sca.4950170309>
- Mojzes, Á. (2009). Using Degradable Foam Cushioning in a Product – Packaging System. *Acta Technica Jaurinensis*, 2(3), 477–491. <https://acta.sze.hu/index.php/acta/article/view/202>
- Mudgil, D., Barak, S., & Khatkar, B. S. (2014). Guar gum: processing, properties and food applications—A Review. *Journal of Food Science and Technology*, 51(3), 409–418. <https://doi.org/10.1007/s13197-011-0522-x>
- Myllytie, P., Salmi, J., & Laine, J. (2009). The influence of pH on the adsorption and interaction of chitosan with cellulose. *BioResources*, 4(4), 1647–1662.
- Neimo, L. (1999). *Papermaking Chemistry (Vol. 4)*. Fapet OY.

- O'Sullivan, J. D. B., Behnsen, J., Starborg, T., MacDonald, A. S., Phythian-Adams, A. T., Else, K. J., Cruickshank, S. M., & Withers, P. J. (2018). X-ray micro-computed tomography (μ CT): an emerging opportunity in parasite imaging. *Parasitology*, 145(7), 848–854. <https://doi.org/10.1017/S0031182017002074>
- Ottenhall, A., Seppänen, T., & Ek, M. (2018). Water-stable cellulose fiber foam with antimicrobial properties for bio based low-density materials. *Cellulose*, 25(4), 2599–2613. <https://doi.org/10.1007/s10570-018-1738-y>
- Paunonen, S., Timofeev, O., Torvinen, K., Turpeinen, T., & Ketoja, J. (2018). Improving Compression Recovery of Foam-formed Fiber Materials. *BioResources*, 13(2), 4058–4074. <https://doi.org/10.15376/biores.13.2.4058-4074>
- Pöhler, T., Ketoja, J. A., Lappalainen, T., Luukkainen, V.-M., Nurminen, I., Lahtinen, P., & Torvinen, K. (2020). On the strength improvement of lightweight fibre networks by polymers, fibrils and fines. *Cellulose*, 27(12), 6961–6976. <https://doi.org/10.1007/s10570-020-03263-x>
- Poranen, J., Kiiskinen, H., Salmela, J., Asikainen, J., Keränen, J., & Pääkkönen, E. (2013). Breakthrough in papermaking resource efficiency with foam forming. Paper Conference and Trade Show, PaperCon, 807–814.
- Punton, V. W. (1975). The use of an aqueous foam as a fibre-suspending medium in quality papermaking. Ed. Akers R.J. *Foams*.
- Robinson, J. V. (1980). Fiber Bonding. In J. P. Casey (Ed.), *Pulp and Paper. Chemistry and Chemical Technology* (Vol. 2, pp. 915–963). Wiley & Sons.
- Roy Choudhury, A. K. (2013). 15 - Process control in finishing of textiles. In A. Majumdar, A. Das, R. Alagirusamy, & V. K. Kothari (Eds.), *Process Control in Textile Manufacturing* (pp. 363–427). Woodhead Publishing. <https://doi.org/https://doi.org/10.1533/9780857095633.3.363>
- Schmied, F. J., Teichert, C., Kappel, L., Hirn, U., & Schennach, R. (2012). Joint strength measurements of individual fiber-fiber bonds: An atomic force microscopy based method. *Review of Scientific Instruments*, 83(7), 073902. <https://doi.org/10.1063/1.4731010>
- Schramm, L. L., & Wassmuth, F. (1994). *Foams: Basic Principles*. In *Foams: Fundamentals and Applications in the Petroleum Industry* (Vol. 242, pp. 3–45). American Chemical Society. <https://doi.org/doi:10.1021/ba-1994-0242.ch001>
- Seo, K. S., Lee, J. C., Bang, K. S., Han, H. S., Chung, S. H., Choi, B. I., & Ha, J. H. (2004, June). Shock absorbing evaluation of the rigid polyurethane foam and styrofoam applied to a small transportation package.
- Smith, M. K., & Punton, V. W. (1975). Foam can improve formation. *Pulp Paper Canada*, 76(2), 114–117.

- Smith, M. K., Punton, V. W., & Rixson, A. G. (1974). The structure and properties of paper formed by a foaming process. *Tappi*, 57(1), 107–111.
- Sotoodeh, K. (2021). 1 - Terms and definitions. In K. Sotoodeh (Ed.), *Prevention of Valve Fugitive Emissions in the Oil and Gas Industry* (pp. 1–35). Gulf Professional Publishing. <https://doi.org/https://doi.org/10.1016/B978-0-323-91862-6.00004-6>
- Strand, A., Kouko, J., Oksanen, A., Salminen, K., Ketola, A., Retulainen, E., & Sundberg, A. (2019). Enhanced strength, stiffness and elongation potential of paper by spray addition of polysaccharides. *Cellulose*, 26(5), 3473–3487. <https://doi.org/10.1007/s10570-019-02308-0>
- Torvinen, K., & Lahtinen, P. (2015). The benefit of cellulose nanofibrils (CNF) to foam formed paper properties. 2015 TAPPI International Conference on Nanotechnology for Renewable Materials Proceedings.
- Venkatarajan, S., & Athijayamani, A. (2021). An overview on natural cellulose fiber reinforced polymer composites. *Materials Today: Proceedings*, 37, 3620–3624. <https://doi.org/10.1016/j.matpr.2020.09.773>
- Vishtal, A., & Retulainen, E. (2014a). Improving the extensibility, wet web and dry strength of paper by addition of agar. *Nordic Pulp & Paper Research Journal*, 29(3), 434–443. <https://doi.org/doi:10.3183/npprj-2014-29-03-p434-443>
- Vishtal, A., & Retulainen, E. (2014b). The improvement of paper extensibility, wet and dry strength by spray addition of agar solutions. *Nordic Pulp and Paper Research Journal*, 29, 434–444.
- Wu, M., Yu, G., Chen, W., Dong, S., Wang, Y., Liu, C., & Li, B. (2022). A pulp foam with highly improved physical strength, fire-resistance and antibiosis by incorporation of chitosan and CPAM. *Carbohydrate Polymers*, 278, 118963. <https://doi.org/https://doi.org/10.1016/j.carbpol.2021.118963>
- Zehnder, A. T. (2013). Modes of Fracture. In *Encyclopedia of Tribology* (pp. 2292–2295). Springer US. https://doi.org/10.1007/978-0-387-92897-5_258
- Zhang, X., Teng, Z., Huang, R., & Catchmark, J. (2020). Biodegradable Starch/Chitosan Foam via Microwave Assisted Preparation: Morphology and Performance Properties. *Polymers*, 12(11), 2612. <https://doi.org/10.3390/polym12112612>
- Zia, K. M., Tabasum, S., Nasif, M., Sultan, N., Aslam, N., Noreen, A., & Zuber, M. (2017). A review on synthesis, properties and applications of natural polymer based carrageenan blends and composites. *International Journal of Biological Macromolecules*, 96, 282–301. <https://doi.org/10.1016/j.ijbiomac.2016.11.095>
- Zweifel, H., Maier, R. D., & Schiller, M. (2009). *Plastics Additives Handbook* (6th ed.). Hanser Publications.

APPENDICES

A. Densities and foaming times of samples

Table A1. Foaming times of samples varied from 11 to 22 minutes, and densities varied from 60.3 kg/m³ to 75.1 kg/m³.

Sample ID	Foaming time (min)	Density (kg/m ³)
old A1	15	63.9
old A2	17	60.6
new A1	20	65.8
new A2	20	61.9
A3	16	67.3
A4	16	60.3
SL1	13	65.7
SL2	14	66.2
HC1	14	70.3
HC2	12	73.2
HC3	12	75.1
KC1	18	71.8
KC2	18	71.6
KC3	14	73.2
KC4	11	61.1
C1	22	64.7
C2	21	68.4
C3	21	70.1
G1	11	56.5
G2	16	64.9
G3	15	68.9
G4	20	65.9
G5	20	57.7
G6	20	66.6
G7	16	64.3
G8	22	60.7

B. Results of Maximum G values

Table B1. Results of maximum G values after the first drop.

Sample ID	Density (kg/m ³)	Max G after 1st drop (Average of 3 samples)	Max G of 1. sample	Max G of 2. sample	Max G of 3. sample	Standard deviation (of 3 samples)
A1	66	72.6	71.8	72.4	73.5	0.7
A2	62	60.3	56.5	60.2	64.2	3.1
A3	67	62.7	60.3	62.3	65.4	2.1
A4	60	69.7	68.9	70.0	70.2	0.6
SL1	66	82.4	71.3	76.7	99.3	12.1
SL2	66	112.7	102.0	115.9	120.1	7.7
HC1	70	76.4	70.5	72.8	86.0	6.8
HC2	73	75.2	64.8	73.1	87.8	9.5
HC3	75	71.0	67.9	68.4	76.6	4.0
KC1	72	65.3	63.3	65.4	67.1	1.6
KC2	72	60.8	54.0	61.6	66.8	5.3
KC3	73	59.4	57.8	60.2	60.2	1.1
KC4	61	71.9	65.1	71.4	79.1	5.7
C1	65	88.5	83.4	84.3	97.9	6.6
C2	68	105.0	79.7	109.5	126.0	19.2
C3	70	103.4	95.7	107.3	107.4	5.5
G1	56	60.4	58.7	59.5	63.0	1.9
G2	65	72.8	70.9	74.7	106.8	16.1
G3	69	77.3	73.3	78.5	80.2	2.9
G4	66	83.2	78.8	-	87.6	4.4
G5	58	69.7	67.6	70.2	71.4	1.6
G6	67	72.9	66.5	75.5	76.8	4.6
G7	64	73.9	64.4	70.4	86.9	9.5
G8	61	70.0	65.8	69.7	74.4	3.5

Table B2. Results of maximum G values after the third drop.

Sample ID	Density (kg/m ³)	Max G after 3rd drop (Average of 3 samples)	Max G of 1. sample	Max G of 2. sample	Max G of 3. sample	Standard deviation (of 3 samples)
A1	66	93.8	92.6	93.4	95.5	1.2
A2	62	94.3	88.2	95.0	99.6	4.7
A3	67	89.5	89.5	92.0	87.0	2.0
A4	60	103.1	98.2	103.7	107.5	3.8
SL1	66	93.3	88.6	97.5	93.8	3.7
SL2	66	100.9	104.1	101.4	97.2	2.8
HC1	70	97.4	96.6	97.8	97.7	0.5
HC2	73	98.6	90.3	101.3	104.2	6.0
HC3	75	95.9	96.0	95.0	96.8	0.7
KC1	72	91.5	93.0	91.6	89.8	1.3
KC2	72	81.4	81.8	86.6	75.8	4.4
KC3	73	86.3	81.5	87.0	90.5	3.7
KC4	61	99.6	100.3	99.0	99.5	0.5
C1	65	108.1	111.4	106.5	106.3	2.4
C2	68	111.2	122.5	116.0	95.1	11.7
C3	70	112.0	117.0	110.3	108.8	3.6
G1	56	93.2	91.0	91.9	96.6	2.5
G2	65	113.0	123.3	113.4	102.2	8.6
G3	69	105.7	104.5	104.0	108.6	2.1
G4	66	104.6	105.7	105.5	103.4	1.0
G5	58	108.3	110.4	106.8	107.8	1.5
G6	67	100.9	101.0	99.5	102.2	1.1
G7	64	93.4	91.7	89.7	98.9	4.0
G8	61	102.4	104.3	104.4	98.5	2.8

C. Results of Resilience

Table C1. Results of resilience after the first drop.

Sample ID	Density (kg/m ³)	Resilience after 1st drop (Average of 3 samples)	Resilience of 1. sample	Resilience of 2. sample	Resilience of 3. sample	Standard deviation (of 3 samples)
A1	66	96.33 %	96.60 %	96.47 %	95.94 %	0.285 %
A2	62	95.43 %	95.46 %	95.44 %	95.40 %	0.023 %
A3	67	96.25 %	95.84 %	96.62 %	96.29 %	0.320 %
A4	60	94.88 %	95.59 %	94.82 %	94.22 %	0.561 %
SL1	66	96.61 %	96.01 %	96.43 %	97.38 %	0.574 %
SL2	66	95.43 %	96.31 %	96.90 %	96.65 %	0.244 %
HC1	70	95.80 %	96.28 %	95.38 %	95.74 %	0.371 %
HC2	73	96.48 %	95.67 %	94.85 %	98.92 %	1.759 %
HC3	75	95.82 %	95.78 %	95.89 %	95.79 %	0.050 %
KC1	72	95.54 %	96.23 %	94.80 %	95.58 %	0.584 %
KC2	72	96.91 %	97.10 %	97.43 %	96.19 %	0.525 %
KC3	73	94.77 %	95.73 %	95.45 %	93.14 %	1.160 %
KC4	61	97.12 %	97.47 %	97.10 %	96.80 %	0.274 %
C1	65	96.89 %	97.22 %	96.69 %	96.76 %	0.236 %
C2	68	97.76 %	98.42 %	98.48 %	96.39 %	0.968 %
C3	70	96.35 %	96.58 %	96.05 %	96.43 %	0.222 %
G1	56	95.08 %	95.83 %	94.72 %	94.69 %	0.530 %
G2	65	95.95 %	95.58 %	96.20 %	96.06 %	0.264 %
G3	69	95.62 %	97.29 %	95.83 %	93.73 %	1.464 %
G4	66	95.07 %	94.51 %	95.57 %	95.14 %	0.434 %
G5	58	92.45 %	91.85 %	93.05 %	92.46 %	0.490 %
G6	67	93.90 %	94.19 %	93.11 %	94.41 %	0.571 %
G7	64	94.85 %	93.60 %	96.30 %	94.63 %	1.113 %
G8	61	95.77 %	94.40 %	96.14 %	96.78 %	1.008 %

Table C2. Results of resilience after the third drop.

Sample ID	Density	Resilience after 3rd drop (Average of 3 samples)	Resilience of 1. sample	Resilience of 2. sample	Resilience of 3. sample	Standard deviation (of 3 samples)
A1	66	93.78 %	93.94 %	93.87 %	93.52 %	0.182 %
A2	62	92.66 %	92.72 %	92.80 %	92.46 %	0.146 %
A3	67	93.65 %	93.75 %	93.25 %	93.96 %	0.302 %
A4	60	92.72 %	92.34 %	93.27 %	92.55 %	0.400 %
SL1	66	95.24 %	93.01 %	96.56 %	96.14 %	1.583 %
SL2	66	95.24 %	94.58 %	96.66 %	-	1.037 %
HC1	70	92.04 %	92.11 %	91.31 %	92.70 %	0.570 %
HC2	73	93.47 %	92.52 %	91.78 %	96.11 %	1.892 %
HC3	75	93.82 %	94.79 %	93.30 %	93.37 %	0.684 %
KC1	72	92.60 %	93.44 %	91.97 %	92.38 %	0.615 %
KC2	72	94.00 %	94.71 %	94.39 %	92.90 %	0.789 %
KC3	73	91.05 %	89.98 %	91.85 %	91.32 %	0.786 %
KC4	61	94.17 %	95.64 %	94.32 %	92.56 %	1.260 %
C1	65	95.57 %	95.17 %	95.87 %	95.66 %	0.294 %
C2	68	96.17 %	96.68 %	96.81 %	95.01 %	0.817 %
C3	70	95.96 %	95.98 %	95.85 %	96.04 %	0.076 %
G1	56	92.00 %	93.26 %	90.82 %	91.91 %	1.002 %
G2	65	92.59 %	91.46 %	92.32 %	93.98 %	1.048 %
G3	69	93.86 %	95.39 %	93.19 %	93.01 %	1.080 %
G4	66	94.86 %	93.48 %	96.10 %	95.00 %	1.075 %
G5	58	90.64 %	89.58 %	90.84 %	91.49 %	0.791 %
G6	67	93.05 %	93.50 %	92.59 %	93.06 %	0.371 %
G7	64	93.34 %	92.44 %	94.65 %	92.94 %	0.944 %
G8	61	93.62 %	92.84 %	93.90 %	94.13 %	0.561 %

D. Results of strain

Table D1. Results of strain after the first drop.

Sample ID	Density	Strain after 1st drop (average of all samples)	Strain of 1. sample	Strain of 2. sample	Strain of 3. sample	Standard deviation of 3 samples
A1	66	34.86 %	33.44 %	30.63 %	40.52 %	4.161 %
A2	62	36.77 %	35.99 %	36.01 %	38.31 %	1.090 %
A3	67	38.59 %	41.54 %	38.14 %	36.09 %	2.250 %
A4	60	44.89 %	45.86 %	44.21 %	44.58 %	0.705 %
SL1	66	36.84 %	37.69 %	37.32 %	35.51 %	0.951 %
SL2	66	34.20 %	32.02 %	36.49 %	34.07 %	1.826 %
HC1	70	39.19 %	42.59 %	40.95 %	34.03 %	3.708 %
HC2	73	43.48 %	46.11 %	41.63 %	42.70 %	1.909 %
HC3	75	32.74 %	33.23 %	29.66 %	35.33 %	2.342 %
KC1	72	39.41 %	41.26 %	40.26 %	36.70 %	1.953 %
KC2	72	38.71 %	40.07 %	37.53 %	38.51 %	1.045 %
KC3	73	44.00 %	46.03 %	40.82 %	45.16 %	2.281 %
KC4	61	40.50 %	41.52 %	40.54 %	39.44 %	0.846 %
C1	65	39.21 %	37.87 %	36.30 %	43.46 %	3.072 %
C2	68	26.59 %	24.38 %	24.30 %	31.08 %	3.177 %
C3	70	30.39 %	27.30 %	32.05 %	31.82 %	2.187 %
G1	56	45.46 %	42.22 %	48.61 %	45.56 %	2.608 %
G2	65	39.69 %	41.85 %	42.38 %	34.85 %	3.430 %
G3	69	33.20 %	32.42 %	33.18 %	33.99 %	0.639 %
G4	66	34.46 %	36.06 %	32.38 %	34.93 %	1.539 %
G5	58	48.82 %	51.16 %	47.53 %	47.77 %	1.657 %
G6	67	40.66 %	41.96 %	38.93 %	41.08 %	1.274 %
G7	64	37.41 %	37.87 %	35.55 %	38.80 %	1.367 %
G8	61	40.22 %	40.87 %	44.00 %	35.78 %	3.384 %

Table D2. Results of strain after the third drop.

Sample ID	Density	Strain after 3rd drop (Average of 3 samples)	Strain of 1. sample	Strain of 2. sample	Strain of 3. sample	Standard deviation of 3 samples
A1	66	38.08 %	38.53 %	46.06 %	3.661 %	38.08 %
A2	62	42.39 %	42.94 %	44.34 %	0.821 %	42.39 %
A3	67	48.73 %	43.62 %	41.42 %	3.061 %	48.73 %
A4	60	52.42 %	47.94 %	48.87 %	1.929 %	52.42 %
SL1	66	42.83 %	44.83 %	43.78 %	0.818 %	42.83 %
SL2	66	35.79 %	41.32 %	40.33 %	2.411 %	35.79 %
HC1	70	46.66 %	44.28 %	39.63 %	2.919 %	46.66 %
HC2	73	48.21 %	42.30 %	46.25 %	2.457 %	48.21 %
HC3	75	37.46 %	34.45 %	40.57 %	2.500 %	37.46 %
KC1	72	44.98 %	46.64 %	43.44 %	1.307 %	44.98 %
KC2	72	46.16 %	42.65 %	45.97 %	1.609 %	46.16 %
KC3	73	54.44 %	43.70 %	49.35 %	4.386 %	54.44 %
KC4	61	45.27 %	48.01 %	48.68 %	1.474 %	45.27 %
C1	65	41.61 %	38.59 %	47.40 %	3.656 %	41.61 %
C2	68	33.18 %	28.04 %	36.54 %	3.493 %	33.18 %
C3	70	33.51 %	33.37 %	36.19 %	1.300 %	33.51 %
G1	56	52.34 %	50.94 %	49.74 %	1.065 %	52.34 %
G2	65	45.65 %	46.67 %	38.90 %	3.448 %	45.65 %
G3	69	35.80 %	39.30 %	38.46 %	1.490 %	35.80 %
G4	66	39.31 %	34.98 %	41.17 %	2.595 %	39.31 %
G5	58	52.36 %	52.19 %	52.79 %	0.252 %	52.36 %
G6	67	49.98 %	45.11 %	46.77 %	2.022 %	49.98 %
G7	64	44.72 %	41.68 %	42.48 %	1.288 %	44.72 %
G8	61	49.15 %	49.98 %	44.34 %	2.485 %	49.15 %

E. Results of maximum displacement

Table E1. Results of maximum displacement after the first drop.

Sample ID	Density	Max displacement after 1 st drop (average of 3 samples, mm)	Max displacement of 1. sample (mm)	Max displacement of 2. sample (mm)	Max displacement of 3. sample (mm)	Standard deviation of 3 samples (mm)
A1	66	17.7	17.0	15.5	20.5	2.1
A2	62	18.5	18.0	18.0	19.5	0.7
A3	67	19.8	21.5	19.0	19.0	1.2
A4	60	22.3	23.0	22.0	22.0	0.5
SL1	66	17.8	18.5	18.0	17.0	0.6
SL2	66	16.8	15.0	17.0	18.5	1.4
HC1	70	19.2	21.0	20.0	16.5	1.9
HC2	73	20.5	23.0	19.5	19.0	1.8
HC3	75	16.7	17.0	15.0	18.0	1.2
KC1	72	19.3	20.0	20.0	18.0	0.9
KC2	72	19.7	20.0	19.0	20.0	0.5
KC3	73	21.3	22.0	20.0	22.0	0.9
KC4	61	19.8	20.0	20.0	19.5	0.2
C1	65	19.7	19.0	18.0	22.0	1.7
C2	68	13.0	12.0	12.0	15.0	1.4
C3	70	14.8	13.5	15.5	15.5	0.9
G1	56	22.5	21.0	24.0	22.5	1.2
G2	65	18.8	19.5	20.0	17.0	1.3
G3	69	16.5	16.0	17.0	16.5	0.4
G4	66	16.2	16.5	15.5	16.5	0.5
G5	58	23.7	25.0	23.0	23.0	0.9
G6	67	19.8	20.5	19.0	20.0	0.6
G7	64	18.7	19.0	18.0	19.0	0.5
G8	61	19.3	20.0	21.0	17.0	1.7

Table E2. Results of maximum displacement after the third drop.

Sample ID	Density	Max displacement after 3 rd drop (average of 3 samples, mm)	Max displacement of 1. sample (mm)	Max displacement of 2. sample (mm)	Max displacement of 3. sample (mm)	Standard deviation of 3 samples (mm)
A1	66	19.7	18.5	18.5	22.0	1.6
A2	62	20.3	20.0	20.0	21.0	0.5
A3	67	21.5	23.5	20.5	20.5	1.4
A4	60	23.2	24.5	22.5	22.5	0.9
SL1	66	20.2	20.0	20.5	20.0	0.2
SL2	66	17.5	16.0	18.5	18.0	1.1
HC1	70	19.8	21.5	20.0	18.0	1.4
HC2	73	20.3	22.5	18.5	20.0	1.6
HC3	75	18.0	18.0	16.5	19.5	1.2
KC1	72	20.7	20.5	21.5	20.0	0.6
KC2	72	21.7	22.0	20.5	22.5	0.8
KC3	73	22.0	24.0	20.0	22.0	1.6
KC4	61	22.0	21.0	22.5	22.5	0.7
C1	65	20.5	20.0	18.5	23.0	1.9
C2	68	15.5	16.0	13.5	17.0	1.5
C3	70	16.2	16.0	15.5	17.0	0.6
G1	56	23.7	24.5	23.5	23.0	0.6
G2	65	19.5	20.0	20.5	18.0	1.1
G3	69	17.8	17.0	19.0	17.5	0.8
G4	66	17.2	17.0	16.0	18.5	1.0
G5	58	23.5	23.5	23.5	23.5	0.0
G6	67	21.7	23.0	20.5	21.5	1.0
G7	64	20.2	21.0	20.0	19.5	0.6
G8	61	21.7	22.5	22.5	20.0	1.2

F. Results of strength and resilience – EPS and PU

Table F1. Results of maximum G values for EPS and PU references.

Sample ID	Density (kg/m ³)	Max G after the 1 st drop	Standard deviation of Max G after the 1 st drop	Max G after the 3 rd drop	Standard deviation of Max G after the 3 rd drop
PU-ref	28	42.9	0.4	52.4	0.7
EPS-ref	20	184.4	0.3	178.7	6.0

Table F2. Results of resilience for EPS and PU references.

Sample ID	Density (kg/m ³)	Resilience after the 1 st drop (%)	Standard deviation of resilience after the 1 st drop (%)	Resilience after the 3 rd drop (%)	Standard deviation of resilience after the 3 rd drop (%)
PU-ref	28	99.35 %	0.25 %	99.12 %	0.33 %
EPS-ref	20	98.73 %	0.15 %	97.23 %	0.03 %

G. High speed camera pictures from Drop test – Maximum displacement

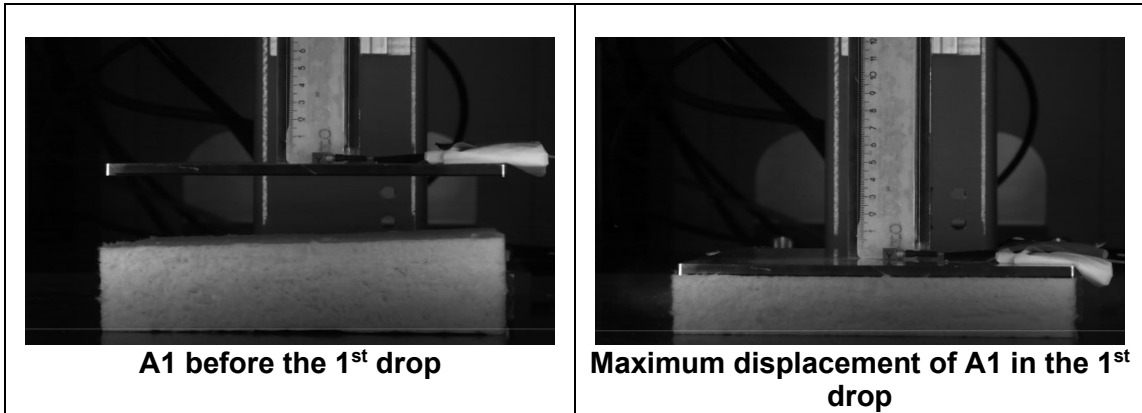


Figure G1. Maximum displacement of reference sample A1.

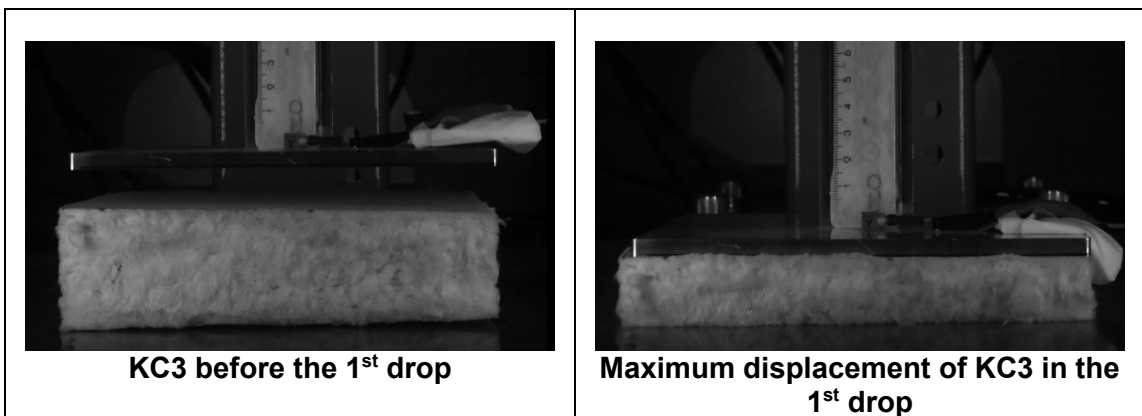


Figure G2. Maximum displacement of sample KC3 with highest maximum displacement out of all samples.

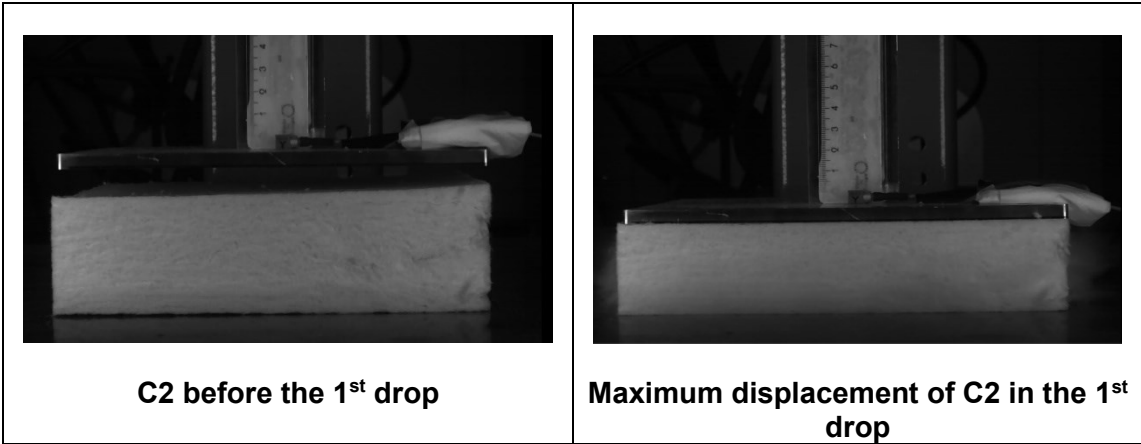


Figure G3. Maximum displacement of sample C2 with lowest maximum displacement out of all samples.

H. High speed camera pictures from Drop test – failure modes

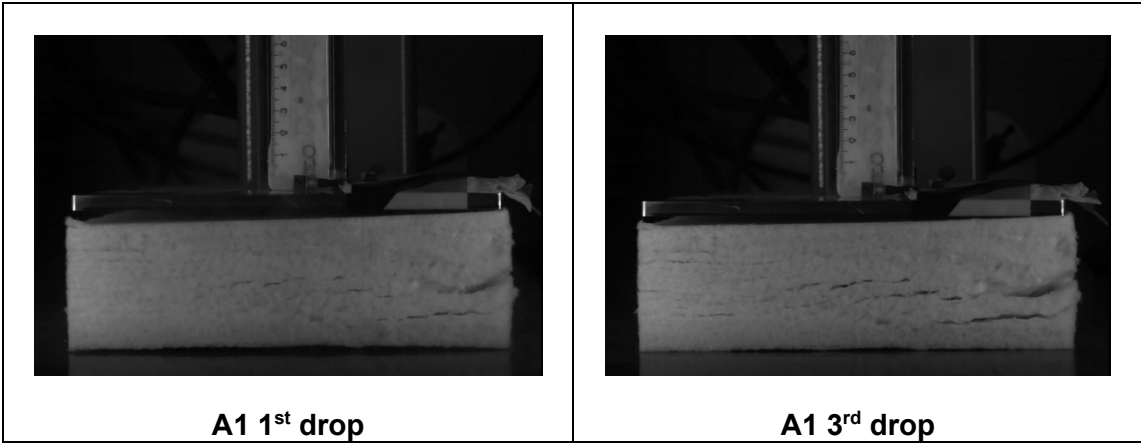


Figure H1. Failure modes of A1 after the 1st and 3rd drops.

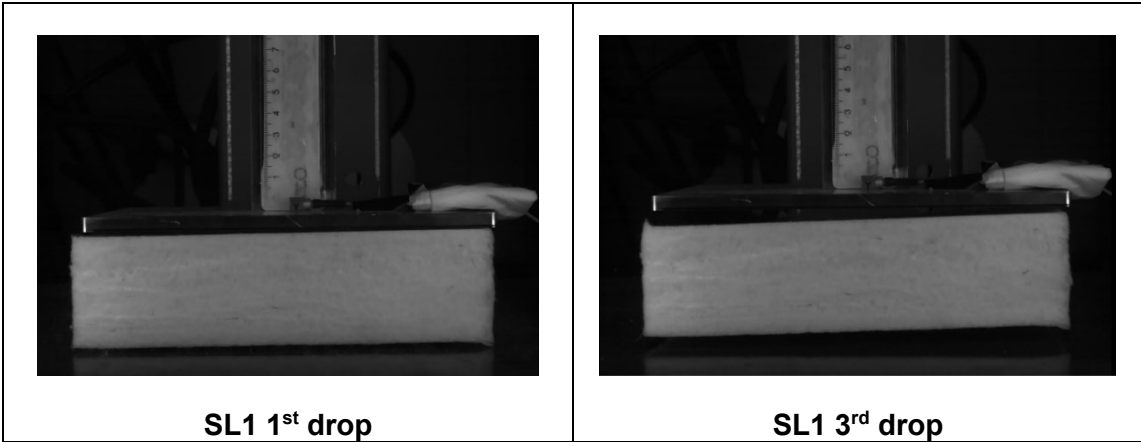


Figure H2. Failure modes of SL1 after the 1st and 3rd drops.

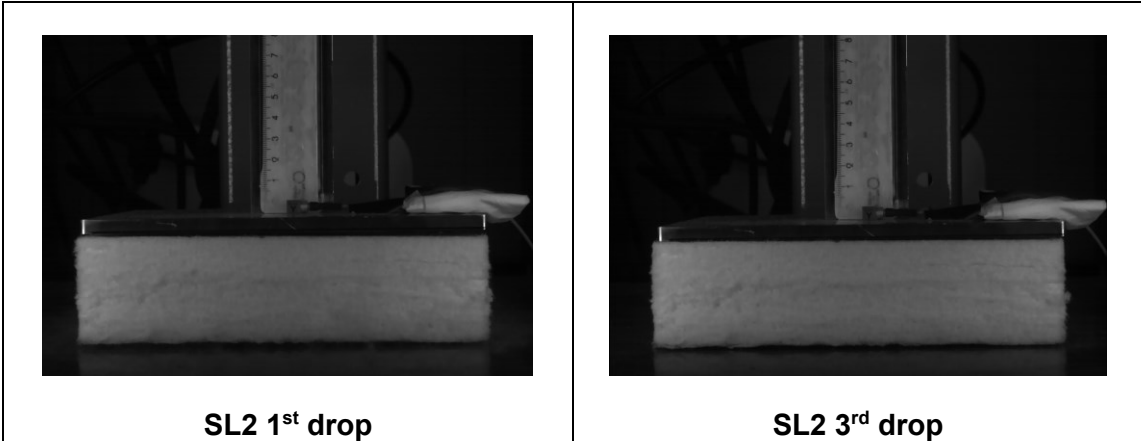


Figure H3. Failure modes of SL2 after the 1st and 3rd drops.

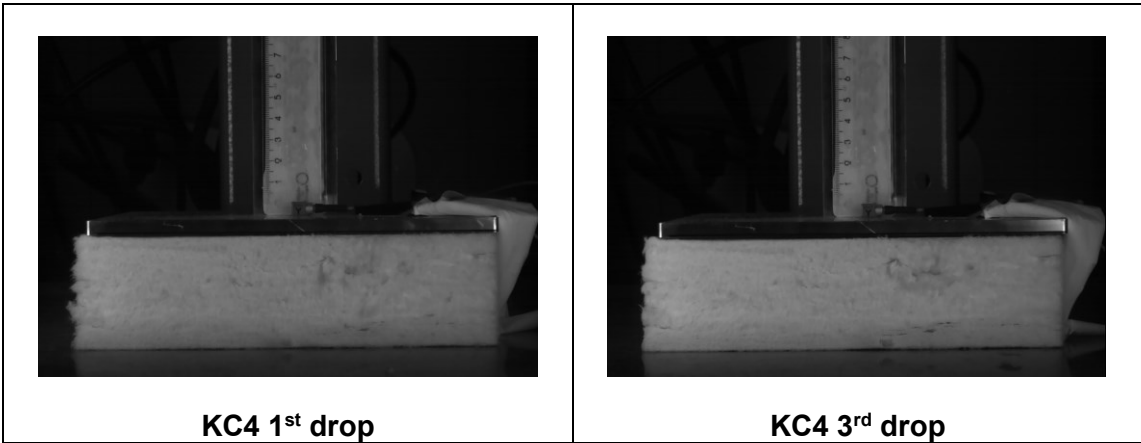


Figure H4. Failure modes of KC4 after the 1st and 3rd drops.

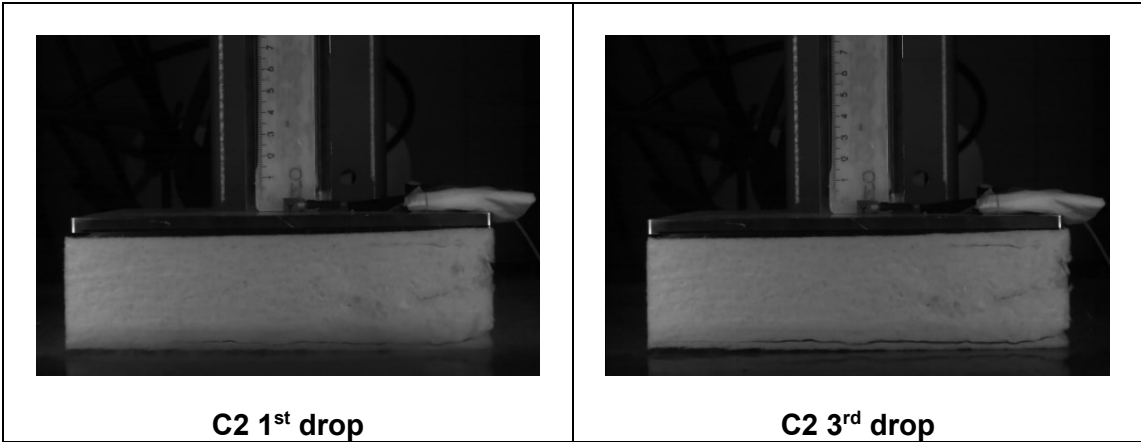


Figure H5. Failure modes of C2 after the 1st and 3rd drops.

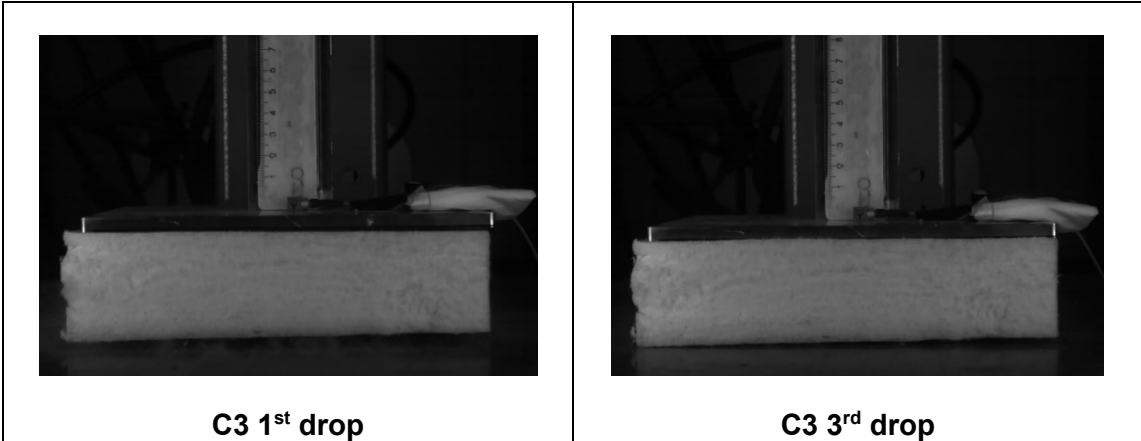


Figure H6. Failure modes of C3 after the 1st and 3rd drops.